Biogeosciences Discuss., 10, 591–641, 2013
www.biogeosciences-discuss.net/10/591/2013/
doi:10.5194/bgd-10-591-2013

Biogeosciences Discussions

Downward fluxes of sinking particulate matter in the deep Ionian Sea (NESTOR site), Eastern Mediterranean: seasonal and interranual variability

S. Stavrakakis, A. Gogou, E. Krasakopoulou, A. P. Karageorgis, H. Kontoyiannis, G. Rousakis, D. Velaoras, L. Perivoliotis, G. Kambouri, I. Stavrakaki, and V. Lykousis

Hellenic Centre for Marine Research (HCMR), Institute of Oceanography, 46.7 km Athens-Sounio Av., 19013 Anavyssos, Greece

Received: 30 November 2012 – Accepted: 10 December 2012 – Published: 10 January 2013

Correspondence to: S. Stavrakakis (stavrak@hcmr.gr), A. Gogou (agogou@hcmr.gr)

Published by Copernicus Publications on behalf of the European Geosciences Union.

Downward fluxes of sinking particulate matter in the deep Ionian Sea

S. Stavrakakis et al.

Abstract

In order to assess seasonal and interranual variability in the export of particulate matter and its main constituents, sediment traps were deployed at five successive depths from February 2006 to March 2010 in the deepest basin of the Mediterranean (SE Ionian Sea, NESTOR site).

The average total mass fluxes were 66, 58, 54, 34, and 52 mg $m^{-2} d^{-1}$, at 700, 1200, 2000, 3200, and 4300 m, respectively. The interranual variability generally witnesses a gradual increase of fluxes during the experiment. The temporal variations of the mass flux showed similar seasonal signal at all sampling depths with higher values in spring–summer and lower in autumn–winter. Changes in the main constituents of the mass flux (organic carbon, carbonates, opal, and lithogenic matter) largely followed the same temporal variability with mass flux, revealing mechanisms of rapid vertical (top-down) transport from 700 m down to 4300 m-depth. Lateral inputs at the deepest trap are probably of importance, attributed to the influence of the deep Adriatic water, characterized by relatively higher turbidity than overlying water masses.

The Ionian Sea displays high seasonal variability with maximum productivity rates observed during the late winter/spring convective mixing period. Our flux study proposes two additional processes, potentially of high importance for fuelling surface waters with nutrients at the NESTOR site: (1) the upwelling of intermediate waters in late spring-early summer, causing nutrient inputs in the surface layer which may lead to episodes of increased productivity, as witnessed by the organic carbon, carbonate, and opal fluxes in the mesopelagic and bathypelagic layers and (2) the influence of episodic dust input events, leading to enhanced fluxes of lithogenic matter.

1 Introduction

Formation and sinking of particulate matter drive the biological carbon pump via export and sedimentation of organic matter from the surface mixed layer to the deep ocean and sediments (reviewed by Honjo et al., 2008). Biotic processes that form, change, transport, and remineralize particulate organic carbon, opal, calcium carbonate, and other minor chemical species in the water column are central to the ocean's biogeochemical cycles and are of fundamental importance to the global carbon cycle (Armstrong et al., 2002; Broecker and Peng, 1982; Lee et al., 2009; Passow, 2004; Volk and Hoffert, 1985).

As the environmental and oceanographic conditions can change substantially over time, time-series studies of particle fluxes as recorded by sediment traps, have been proved valuable for biogeochemical studies in the world ocean (Buesseler et al., 2007; Buesseler and Boyd, 2009; Conte et al., 2001; Fabres et al., 2008; Haake et al., 1993; Honda et al., 1997; Honjo et al., 2008; Ittekkot et al., 1992; Karl et al., 1996, 2001; Lee et al., 2009; Martin et al., 2010; Sanchez-Vidal et al., 2005; Takahashi et al., 2000, 2002; Wong et al., 1999; Zuniga et al., 2007). The fraction of organic matter that sinks out from the upper mixed layer of the ocean is, among other factors, determined by the sinking velocity and microbial remineralization rates of marine aggregates, fecal pellets and carcasses of different organisms, feeding the vertical flux of organic material. During intense bloom periods, phytoplankton can contribute a significant part of the flux through direct sedimentation, without being grazed by zooplankton. Overall, open ocean flux of organic carbon rarely exceeds 0.1–2 % of the net primary production below 2000 m (Lampitt and Antia, 1997). Processes of particle dissolution and remineralization are very intense during transport in the water column and the sea floor, and most particulate organic carbon is returned to inorganic form and redistributed in the water column, determining the surface concentration of CO_2, and hence the rate at which the ocean can absorb CO_2 from the atmosphere. The ability to predict quantitatively the depth profile of carbon remineralization is therefore critical to global change studies (Siegenthaler and Sarmiento, 1993).

The Mediterranean Sea is a marginal sea which has been suggested to play an important role in the drawdown of anthropogenic carbon (Aït-Ameur and Goyet, 2006; Álvarez et al., 2005). Recently published anthropogenic CO_2 (C_{ant}) estimates

BGD
10, 591–641, 2013

(Krasakopoulou et al., 2011; Schneider et al., 2010; Touratier and Goyet, 2011), showed that the C_{ant} inventory for the Mediterranean is ~ 1.7 Pg C, thus indicating that this marginal sea has higher C_{ant} concentrations than the global average, mainly determined by the surprisingly high anthropogenic carbon content of the Eastern Mediterranean Sea (Sabine and Tanhua, 2010; Schneider et al., 2010). The strong uptake of anthropogenic CO_2 by the Mediterranean Sea is mostly driven by its high alkalinity, coupled with the wintertime dense water formation events.

Numerous trap experiments have been carried out over past decades in the Mediterranean, both in continental shelf and open sea environments, concerning mass fluxes, budgets of particulate organic carbon, major and minor elements (Boldrin et al., 2002; Gogou et al., 2012; Lee et al., 2009; Miquel et al., 2011; Sanchez-Vidal et al., 2005; Zuniga et al., 2007) and variability of particle fluxes and mechanisms controlling the transfer of particulate matter to the open sea (Canals et al., 2006; Heussner et al., 2006; Martin et al., 2010; Monaco et al., 1999; Pasqual et al., 2010; Stavrakakis et al., 2000; Stavrakakis and Lykousis, 2011).

The present study focuses on the downward fluxes of the total mass, organic carbon, carbonate, opal, and lithogenic matter during the first long time series (February 2006 to March 2010) collected in the deepest Mediterranean basin (NESTOR site), SE Ionian Sea, in the Eastern Mediterranean. The time-series dataset allows to resolving the seasonal and interranual variability and the background environmental, biogeochemical and oceanographic conditions, which control particle export in the study area. The overall goal is to develop a comprehensive understanding of carbon fluxes and associated mineral ballast fluxes throughout the water column in the NESTOR site area.

BGD
10, 591–641, 2013

2 Study area

2.1 Morphological setting of the study area

NESTOR site is located in the SE Ionian Sea, in the vicinity of SW Peloponnese (Fig. 1). The submarine morphology of the area is complicated with steep slopes close to the Messinia/Pylos, valleys and deep basins. The steep slope extends in short distances from the shore from 600 to 3000 m depth, while further offshore, from 3000 to 4000 m depth, the area is dominated by valleys and morphological plateaus, which incorporate the deepest basins of the Mediterranean Sea (4600 and 5264 m depth).

Detailed continuous sub-bottom seismic profiling revealed that the bottom sediment sequences arevery thin due to the insignificant sediment inputs from the nearby continent. The steep slopes are almost free of sediments (acoustic basement) and the valleys and plateaus are covered by undisturbed sediments (lack of slumps or massive sediment failures). The sub-bottom strata of the deep basins consist of continuous weak and parallel reflectors indicating purely pelagic sedimentation with the absence of turbidity flows (KM3NeT Collaboration, 2007).

2.2 Hydrology and biogeochemistry

The Ionian Sea has a complex hydrology and can be considered as a transitional area where water masses formed in the Levantine, the Aegean Sea and the Adriatic Sea meet and interact with the water masses of the Western Mediterranean Sea that enter through the Sicily Straits. The typical water mass structure of the area includes: (1) the Modified Atlantic Waters (MAW) characterized by a salinity minimum and occupying the approximately upper 25–100 m; (2) the Levantine Intermediate Waters (LIW) that occupy typically the 100–500 m layer and are characterized by a salinity maximum; (3) the Transitional Waters (TW) occupying the layer between 500 and 1200 m; and (4) the Eastern Mediterranean Deep Waters (EMDW) filling the layers below 1200 m (Malanotte-Rizzoli et al., 1997; Nittis et al., 1993). The Eastern Mediterranean Transient

BGD
10, 591–641, 2013

(EMT) of the early 1990s' further complicated this structure (Theocharis et al., 1999). The bottom waters of the Ionian Sea were occupied by the newly formed warm and saline Cretan Deep Water (CDW), which displaced the older EMDW of Adriatic origin (Klein et al., 1999). The intermediate layers were occupied by Cretan Intermediate Waters (CIW) with characteristics similar to LIW (Malanotte-Rizzoli et al., 1999).

New production in the Ionian Sea mostly derives from limited events in space and time which are mainly driven by climatological factors generating mesoscale instabilities (Boldrin et al., 2002; Casotti et al., 2003; Civitarese et al., 2010; Mazzocchi et al., 2003). Oligotrophic features increase according to a north-south and west-east gradient (Bosc et al., 2004; Casotti et al., 2003; D'Ortenzio et al., 2003), in response to different water mass characteristics and circulation patterns. Surface Chl *a* concentrations in the Eastern Ionian are generally lower than 0.2 $mg\,m^{-3}$ with the occurrence of the highest values during late winter and early spring, and the lowest levels during summer (D'Ortenzio et al., 2003). A deep chlorophyll maximum is found at around 80–100 m depth (Boldrin et al., 2002; Casotti et al., 2003; Crombet et al., 2011; Karageorgis et al., 2012; Rabitti et al., 1994) exhibiting low seasonality that is related to the stable oligotrophic conditions of the area (Casotti et al., 2003). In general, previous studies depict that the oligotrophic Ionian Sea is dominated by a complex microbial food web (review by Siokou et al., 2010; Yokokawa et al., 2010), and dissolved organic matter (DOM) is partially bioavailable in both surface and mesopelagic and bathypelagic layers, as witnessed by the important correlation of DOC with AOU and the chemical characteristics of DOM (Meador et al., 2010).

3 Materials and methods

3.1 Sampling strategy

NESTOR mooring line (4500 m depth) was deployed at the deepest basin of the SE Ionian Sea (36°32.96 N, 21°28.93 E; Fig. 1). The mooring line was instrumented with five pairs of sediment traps (TECHNICAP PPS3/3, 0.125 m^2 collecting area and 12 receiving cups) and current meters (AANDERAA RCM-11 and RCM-9). The five traps were set at 700, 1200, 2000, 3200, and 4300 m depth, whereas the current meters were set 3 m below the traps. At the deepest trap of NESTOR site (4300 m), the collection of settling particles started on 18 February 2006. The traps at 1200, 2000 and 3200 m depth commenced sampling on 3 June 2006 and the shallower trap at 700-m-depth on 1 November 2006, with a sampling gap from October 2008 to March 2009. The collecting periods of each trap are summarized in Fig. 2a. All traps were synchronized to collect particles on weekly (1 April 2006–31 May 2006, and 16 August 2006–7 October 2006) or bi-weekly basis. A poisoning solution of formalin (Knauer et al., 1984) was used to limit the degradation of particulate matter and to prevent the integrity of "swimmers" by hardening their cuticle. Details of mooring line preparation and preliminary sample treatment are described by Heussner et al. (1990). The water mass characteristics of the sampling area were recorded by use of a SeaBird CTD sensor.

During the entire sampling period, 399 samples were recovered out of the theoretical maximum of 404 (99 % success rate; Fig. 2a).

3.2 Sample treatment and analytical procedures

The recovered trap samples were kept in the dark at 4 °C, until treated in the laboratory. Part of the supernatant passed through a 1 m nylon sieve, to remove large organisms. Smaller than 1 mm swimmers were removed by hand, under a light microscope using fine tweezers. A high-precision peristaltic, microprocessor-controlled dispensing pump was used to divide the sample into subsamples. Subsamples for the determination of opal (biogenic silica) were filtered onto Millipore 0.45 µm cellulose filters (HA), whereas subsamples for the determination of carbon and nitrogen were filtered onto Whatman glass microfibre filters (GF/F). Total mass fluxes were calculated from the dry weights of the subsamples used for opal analyses.

BGD
10, 591–641, 2013

For the determination of organic (OC) and total (TC) carbon, subsamples of ∼ 8 mg of sinking matter, were filtered through pre-combusted (450 °C), pre-weighed GF/Filters which then were stored at −20 °C in the dark until analysis. OC and TC contents were measured with a Thermo Scientific FLASH 2000 CHNS elemental analyzer in HCl treated and non-treated samples, respectively (Nieuwenhuize et al., 1994). The analytical conditions are set at provider recommended parameters slightly modified according to the published works of Verardo et al. (1990), Cutter and Radford-Knoery (1991) and Nieuwenhuize et al. (1994). For the elimination of inorganic carbon, filters are firstly treated with HCl 2 N to prevent "explosive" sample loss during reaction with more concentrated acid in the next step, that is consisted by repeated additions of HCl 6 N with 60 °C drying steps in between until no further effervescence is noticed.

From the values obtained, organic matter (OM) content was calculated by doubling the OC content [OM %=OC % × 2], carbonate content was estimated assuming all inorganic carbon [TC %−OC %] was $CaCO_3$ and using the molecular mass ratio 100/12 [(TC %−OC %) × 8.33].

Opal concentration was determined by colorimetric reaction after extraction of silica into 2 M Na_2CO_3 and 2 N NaOH solution at 85 °C for 5 h. According to Mortlock and Froelich (1989) opal contents were obtained by multiplying the values of Si concentration by a factor of 2.4.

The lithogenic fraction (quartz, aluminosilicates, heavy minerals, etc.) was estimated by subtraction of the sum of biogenic components from 100 [lithogenic % = 100 % − (organic matter% + carbonates% + opal%)].

In some cases the limited amount of trapped material was insufficient for the analyses of all constituents; Fig. 2b–e shows the analyses performed for each major constituent.

4 Results

4.1 Hydrodynamic regime

In the framework of the present work, the detailed analysis of the hydrographic and current meter data during 2006–2009 showed that a permanent cyclone was dominant in the deepest ∼ 2–2.5 km, while the flow in the upper ∼ 1.5–2 km was variable. In February and May 2006, the upper flow was to the east and southeast, under the influence of the northern edge of the Pelops anticyclone, while it switched afterwards to the northwest in the absence of the Pelops anticyclone in our study area. In addition, CDW was detected with local maxima of temperature and salinity at ∼ 1600 m and at ∼ 3300 m depth, whereas waters of Adriatic origin existed at depths below ∼ 3600 m. Figure 3 shows the progressive vector diagrams derived from the current meter data at the five instrumented depths of the mooring at NESTOR. The predominant direction of flow at all depths is to the north-northwest towards directions in the range 320–340°. The flow at the deepest level (4300 m) is mostly stable in direction, i.e. along the local bathymetry towards 321° T on average. Fairly stable in direction is also the flow at 2000 m towards ∼ 340° T on average. Higher variability is observed in the shallower flows, i.e. at 700 and 1200 m, which appear to be correlated to each other, i.e. nearly parallel, in the period from May 2006 until March 2008. In April 2008, the flow at 700 m turns to the southwest, whereas the flow at 1200 m turns to the west and ultimately returns back to the northeast in February 2009. Variable flow directions were also observed in the relatively short one-year record at 3200 m. Compared to all recorded flows, the record at 3200 m was the only one that exhibited a flow to the southeast. This occurred in early fall of 2006, before switching to the northwest in February 2007. The speeds of the flows at all levels are extremely weak. Mean speeds are 2.9, 2.8, 1.8, 1.5, and 2.2 $\mathrm{cm\,s^{-1}}$, at 700, 1200, 2000, 3200, and 4300 m, respectively, whereas the corresponding maxima speeds are 12, 18, 9, 9, and 14 $\mathrm{cm\,s^{-1}}$.

BGD
10, 591–641, 2013

4.2 Total mass flux

Time series of total mass fluxes are illustrated in Fig. 4. Mass fluxes range between two or three orders of magnitude at each depth. The lowest value of mass flux is recorded at 4300 m (0.12 $mg\,m^{-2}\,d^{-1}$, December 2010) and the highest at 700 m (484 $mg\,m^{-2}\,d^{-1}$, March 2010). Mean total mass fluxes measured during the experiment are generally low, confirming the oligotrophic character of the area and span over a narrow range, between 66 $mg\,m^{-2}\,d^{-1}$ at 700 m and 34 $mg\,m^{-2}\,d^{-1}$ at 3200 m (Fig. 4; Table 1). Since the coefficients of variation (CV% = std dev/mean*100) of mass fluxes are much higher compared to the coefficients of variation of percentages of major constituents at all depths (Table 2), the temporal evolution of fluxes of major constituents reflects the mass flux pattern. Among all traps, the upper trap shows the highest variability. However, all traps recorded the same seasonal signal with minor exceptions.

Measured mean total mass fluxes are comparable to those reported for other sectors of the Mediterranean Sea. In the central part of the Algero-Balearic Basin, Zúñiga et al. (2007) measured in four sediment traps (250, 845, 1440, and 1820 m) mean total mass fluxes < 400 $mg\,m^{-2}\,d^{-1}$. In the eastern Alboran Sea, Sanchez-Vidal et al. (2004) estimated at several depths (510–2230 m) mean total mass fluxes substantially higher, in the range of ~ 20 to 2400 $mg\,m^{-2}\,d^{-1}$. In the DYFAMED site situated in the Ligurian Sea, Miquel et al. (2011) reported mean total mass flux from minimum values ~ 3 $mg\,m^{-2}\,d^{-1}$ to a maximum of 1228 $mg\,m^{-2}\,d^{-1}$ at 200 m, and 2 to 893 $mg\,m^{-2}\,d^{-1}$ at 1000 m. In the Eastern Mediterranean, Stavrakakis et al. (2000) measured mean total mass fluxes in the Cretan Sea of 187 and 550 $mg\,m^{-2}\,d^{-1}$ at 200 and 1515 m, respectively, whereas Kerhervé et al. (1999), measured in the Antikythira Strait 96 and 299 $mg\,m^{-2}\,d^{-1}$ at 880 and 1345 m depth, respectively. Finally, Boldrin et al. (2002) reported mean fluxes of 106 and 196 $mg\,m^{-2}\,d^{-1}$ at 150 and 1050 m, respectively in the southern Adriatic Sea and 36 and 17 $mg\,m^{-2}\,d^{-1}$ at 150 and 2250 m, respectively in the northern Ionian Sea.

BGD
10, 591–641, 2013

Mass flux close to the bottom is a good indicator of the sedimentation rate, thus, assuming, that the entire amount of particles caught by the trap at 4300 m reaches the seabed, the sedimentation rate in the study site is estimated at 1–1.45 cm kyr^{-1}. This value is in good agreement with sedimentation rates reported earlier for the area, in the order of 0.7–1.8 cm kyr^{-1} (Trimonis and Rudenko, 1993) or 0.86–1.89 cm kyr^{-1} (Polimeris et al., 2009). Additionally, sediment cores collected close to the location of NESTOR site reveal sedimentation rates of 1.6–1.7 cm kyr^{-1} (KM3NeT Collaboration, 2007), which is also in good agreement with those estimated from sediment trap measurements in our study.

4.3 Organic carbon

The time series of the OC contents and fluxes of all measurements are illustrated in Fig. 5 and statistical parameters are reported in Table 2. For a better comparative description, the mean OC contents and fluxes of the common collecting periods are given in Table 3.

The highest variability in terms of OC content is observed at 700 m and 4300 m, where the CV% are 75 and 100, respectively, and the lowest variability at 3200 m (CV% = 39). At 700 m, high OC contents are observed from November 2006 to Ferbuary 2007, where the total mass flux is generally low and the highest peak is observed in November (15.8 %). This November peak is also recorded at the 1200 m and 2000 m traps after two sampling periods. No remarkable maximum is observed at 3200 m, while at the deepest trap the OC% values are generally high, with maxima followed by minima. The next long period between April 2007 and May 2009 is characterized by lower and less variable OC%. Another maximum of OC% appears at 700 m in October/November 2009 (14 %), followed by two other maxima at 1200 m in November (11 %), and at 4300 m in December (9 %). No peak is observed in October/November 2009 at 2000 m and 3200 m. Due to the relatively small variations in OC contents for each trap (CV% ranges between 39 and 100 %) in comparison with the higher variation in total mass fluxes (CV% ranges between 118 and 141 %), the variations in OC fluxes

BGD
10, 591–641, 2013

followed essentially those of the total mass fluxes. This pattern is the same for all major constituents (see below). From the shallower to the deeper trap, the range of OC fluxes were 0.07 (December 2009)–13 (February/March 2010), 0.16 (February 2007)–12.3 (May 2009), 0.09 (September 2008)–11.4 (May 2009), 0.03 (January 2010)–7.7 (May 2009), and 0.01 (December 2009)–9.6 (May 2009) $\text{mg m}^{-2}\,\text{d}^{-1}$. It is noteworthy that (1) OC content peaks only casually coincide with OC flux peaks; and (2) the mean OC fluxes decrease from 700 m to 3200 m, and increase from 3200 m to 4300 m.

4.4 Carbonates

The time series of carbonate contents and fluxes of all measurements are illustrated in Fig. 6 and statistical parameters are reported in Table 2.

Time series of carbonate contents display less variability in comparison with the higher variation of OC contents; this is confirmed by the lower coefficients of variation (Table 2). Mean carbonate contents did not show any trend of increase or decrease with depth. The lower mean carbonate content (26.5 %) is recorded at 3200 m.

Similarly to OC, the small variations in carbonate content follow the total mass flux pattern. Carbonate fluxes vary between 0.34 (December 2009) and 127 (March 2010) at 700 m, 0.33 (November 2009) and 94 (May 2009) at 1200 m, 0.07 (September 2008) and 82 (April 2009) at 2000 m, 0.27 and 60 (May 2009) at 3200 m, and 0.79 (October 2006) and 79 $\text{mg m}^{-2}\,\text{d}^{-1}$ (May 2009) at 4300 m. Mean carbonate fluxes decrease from 700 m to 3200 m and increase from 3200 m to 4300 m following the trends of the total mass flux and the OC flux.

4.5 Opal

The time series of the opal contents and fluxes of all measurements are illustrated in Fig. 7 and statistical parameters are reported in Table 2.

The variations of opal content are more pronounced than the variation of carbonate, and less than those of OC contents. Despite the fluctuation in opal content between

Discussion Paper | Discussion Paper | Discussion Paper | Discussion Paper |

BGD

10, 591–641, 2013

Downward fluxes of sinking particulate matter in the deep Ionian Sea

S. Stavrakakis et al.

samples, at 700 m the opal contents show a gradual increase from November 2006 to October 2008, and afterwards a gradual decrease until August 2008 (Fig. 7). The opal contents increase again throughout May-June-July 2009, where the highest values are recorded (15.5–17 %). A similar feature is observed at 1200 m, but here the major peak of May 2009 is more pronounced (23 %). This trend is less evident at 2000 m and the spring (May–June) maximum is a slightly higher (21.5–24 %). At 3200 m, four main peaks are recorded: (1) in September 2006 (16.5 %); (2) January 2008 (19 %); (3) May 2009 (22 %); and (4) February 2010 (29 %). At 4300 m, the opal content displays the lowest variability. Mean opal contents are very similar at 1200, 2000 and 3200 m (12-13 %), and slightly lower at 700 and 4300 m (10.2 and 10.7 %, respectively).

The opal fluxes vary between 0.3 (November 2006) and 50 (March 2010), 0.1 (December 2006) and 68 (May 2009), 0.4 (September 2008) and 71 (May 2009), 0.4 (February 2008) and 50 (May 2009), 0.2 (March 2007) and 48 mg m^{-2} d^{-1} (June 2009), for 700, 1200, 2000, 3200, and 4300 m, respectively. Inversely to the OC fluxes, the opal fluxes do not exhibit considerable decrease with depth.

4.6 Lithogenic fraction

The time series of the lithogenic contents and fluxes of all measurements are illustrated in Fig. 8, while statistical parameters are reported in Table 2.

Lithogenic constituents represent the major proportion of the total mass flux, with contents varying between 33 and 70 %. Mean contents of the lithogenic fraction remain almost constant at each collecting depth, with a slight trend to increase towards the deeper traps. It is noteworthy, that the CVs% of the lithogenic component are the lowest among the CVs of all other major constituents.

Mean lithogenic fluxes are from top to bottom: 34, 38, 33, 19, and 38 mg m^{-2} d^{-1}. The lithogenic flux patterns follow largely the total mass flux patterns, resulting from the low CVs of lithogenic percentages and the high variations of total mass fluxes. Lithogenic fluxes vary from 2 (October 2007) to 282 (March 2010), 1 (October 2007) to 160 (August 2008), 2 (February 2008) to 159 (May 2009), 1 (January 2008) to 97

BGD
10, 591–641, 2013

(May 2009), and 2 (February 2008) to 166 (June 2009) $mg\,m^{-2}\,d^{-1}$ for 700, 1200, 2000, 3200, and 4300 m, respectively.

5 Discussion

5.1 Vertical fluxes in the deep layers of NESTOR site

Vertical distribution of mean total mass fluxes during the entire four-year experiment show a general decrease with depth, from 700 m downward to 3200 m, whereas at the 4300 m relatively increased fluxes are observed (Fig. 4; Table 1). Karageorgis et al. (2008) studied the seasonal particle dynamics in the NESTOR area by means of transmissometry and showed that the broader NESTOR area is characterized by very low beam attenuation (beam c_p) values, decreasing over depth. Only extremely faint intermediate and benthic nepheloid layers, (INL and BNL, respectively) detaching from the shelf break and slope moving horizontally along isopycnals were recorded, thus feeding the seabed with very small amounts of particulate matter. In both cases, INLs and BNLs were extremely faint and corresponded to very small differences in beam attenuation (Karageorgis, 2007). Thus, the increase of total mass flux from 3200 m down to 4300 m could be either due to resuspension/lateral advection from the slope-margin and/or to the higher turbidity (higher particulate matter concentration) water of Adriatic origin (EMDW), as it was detected at depths below ~ 3600 m (Kontoyiannis and Lykousis, 2011).

A general behavior observed for the total mass flux as well as all measured constituent fluxes is the consistent presence of maxima and minima appearing almost simultaneously at the five traps, though at varying intensity (Figs. 4–8). Such pattern outlines the predominance of vertical transport over lateral inputs of particulate matter in the area, notwithstanding the fact that water masses move much faster laterally (km per day; mean speeds of flows < $3\,cm\,s^{-1}$ (Fig. 2)) than mean particle sinking rates (10 to 100 $m\,d^{-1}$; Buesseler et al., 2007). However, the variability of mass fluxes between

BGD
10, 591–641, 2013

traps occurring during similar times may be attributed to the presence of various water masses of different particulate matter concentrations. Indeed, CDW which occupies waters between 1600 and 3300 m is very transparent, almost particle-free water mass (Karageorgis et al., 2008). The unique character of CDW, in combination with the lowest measured mean speeds of flow (1.5 cm s^{-1}) appearing at the same depth may explain the relatively lower mass fluxes recorded at the 3200 m-trap. In contrast, relatively higher mass fluxes observed at the deeper trap may be attributed to the presence of EMDW, well-known for its higher turbidity (e.g. De Lazzari et al., 1999).

5.2 Seasonal variability

Temporal distribution of total mass flux exhibits strong seasonal patterns, with higher fluxes recorded mainly in late winter/early spring followed by a second, more pronounced flux maximum period in late spring/summer and significantly lower fluxes in autumn/winter (Fig. 4). This oscillation in total mass flux was observed throughout the four-year experiment, although a marked interranual variability in export intensities is observed. Primary productivity in the Ionian Sea, as in most oligotrophic sites of the subtropical Mediterranean Sea, displays high seasonal variability with maximum rates observed during the winter/spring convective mixing period (Bosc et al., 2004; D'Ortenzio and Ribera d'Alcala, 2009). In our time-series, this feature was observed to coincide with relative increases in organic carbon and opal contents and fluxes at all depths during late winter/ early spring (Figs. 5, 7) and could be attributed to the development of siliceous blooms in the euphotic zone. After that, nanophytoplankton species (e.g. coccolithophorides) probably gained more importance as primary producers, as it is witnessed by the increase in the carbonate contents during the less productive periods (Fig. 6). In respect to this finding, Ignatiades et al. (2009) showed that coccolithophores are the main planktonic calcifiers in the Eastern Mediterranean and a major contributor to biogenic particle export production on a seasonal basis (Malinverno et al., 2009; Triantaphyllou et al., 2004).

BGD
10, 591–641, 2013

Title Page
Abstract | Introduction
Conclusions | References
Tables | Figures
◀ | ▶
Back | Close
Full Screen / Esc
Printer-friendly Version
Interactive Discussion

As for mass flux, a second, more pronounced flux maximum period was observed for all biogenic (OC, carbonate, opal) fluxes measured in late spring/summer of each year (May–July; Figs. 5–8), indicating the existence of a triggering process that enhances highest export of all biogenic fluxes during this time. A plausible explanation for that, given that the main blooming period every year occurs in late winter/early spring, could be some physical mechanism that would enrich the euphotic zone with nutrients from e.g. upwelling from subsurface layers and/or the atmosphere.

Regarding the former hypothesis, a contour plot of time series of salinity profiles, obtained from the CT (conductivity, temperature) array in the nearby (36°50.15 N, 21°36.68 E; Fig. 1) observational buoy of the Poseidon system (www.poseidon.hcmr.gr) shows that in May 2008, May 2009 and May 2010 there is an upwelling of waters with high salinities in the LIW layer at ~ 350 m. The high salinity signal of subsurface waters of Levantine/Cretan origin reaches near-surface layers in the euphotic zone (Fig. 9). This upwelling may be enhancing the nutrient content in the euphotic zone and thus causing occasionally increased surface productivity and enhancement in fluxes in the sediment traps.

During the same periods (May–July), the lithogenic fluxes were also considerably high (700 m-trap: 65 and 85 $\mathrm{mg\,m^{-2}\,d^{-1}}$, in 2008 and 2009, respectively), thus indicating enhanced lithogenic inputs (Fig. 8). Since the area is characterized by the absence of important riverine and runoff inputs, the aeolian transport is probably the prevailing process transferring lithogenic material in the marine environment. An increase of aerosol optical depth (a measure of radiation extinction at the encounter of aerosol particles in the atmosphere) above NESTOR site is recorded in satellite images during e.g. April 2008, April 2009, concomitant to the increase of lithogenic content as well the lithogenic flux in the traps could support this hypothesis (Fig. 10).

The majority of dust deposition occurs in episodic events in the Mediterranean, in an eastward increasing gradient, and plays an important role in fueling the surface waters of the Eastern Mediterranean Sea with nutrients, thus having important implications on pelagic productivity and functioning of the food web, Guerzoni et al., 1999; Herut et al., 2002; Kouvarakis et al., 2001; Krom et al., 1991, 2002; Loye-Pilot et al., 1990; Markaki et al., 2003; Ridame and Guieu, 2002; Thingstad and Rassoulzadegan, 1995). However, the intensity of dust inputs does not cause always analogous changes in the content and flux of the lithogenic fraction. This is probably due to the different atmospheric conditions prevailing during the dust loading events in the atmosphere, i.e. wind speed, precipitation. Indeed, strong atmospheric events force deeper convection in a cyclonic structure such as the one reported for the northern Ionian Sea since 1998 (Manca et al., 2003) and produce a larger vertical transport of nutrients in the photic layer, allowing an enhanced plankton growth. The above description is also confirmed by Boldrin et al. (2002) and Patara et al. (2009), who present data of a sediment trap located in the northern Ionian Sea, through the years 1997–1999.

In 2007, a year of relatively low mass flux values compared to the fluxes recorded during the following years the total mass flux peak at 700 m in August coincided with a period of series of massive forest fires, which affected the western and southern Peloponnese (see Theodosi et al., 2012). Thus, elevated total mass fluxes recorded during August 2007 could be related to elevated atmospheric ash fallout. In fact, scanning electron microscope observations revealed ample coal ash, also reported by Theodosi et al. (2012). Considering that many fires may be related to human activities, it should be noted that anthropogenic impacts can be also recorded by sediment traps.

Distinct peaks of total mass fluxes observed at the 700-m trap, are often observed at deeper traps, but with a considerable time offset (Fig. 11). During April 2009, a major peak in total mass flux was recorded by the 700 m trap, which was also observed at all depths with a delay of ~ 15 days between traps. Thus, the peak was recorded at 4300 m in June (Fig. 11). Assuming a total transport time of 45 days, the particle settling velocity would be 60–80 m d^{-1}. This value is lower than previous estimates of 200 m d^{-1} of Patara et al. (2009), who deployed sediment traps at 500 and 2800 m between 1999 and 2001, SW of the NESTOR site.

Discussion Paper | Discussion Paper | Discussion Paper | Discussion Paper |

BGD

10, 591–641, 2013

Downward fluxes of sinking particulate matter in the deep Ionian Sea

S. Stavrakakis et al.

5.3 Interannual variability

A considerable interannual variability in vertical distributions is observed in the total mass flux maxima at various depths, despite some similarities in the seasonal patterns (Fig. 11). The main feature of the mass flux variability (Table 3 and Fig. 11) was the gradual increase of winter mass flux almost at all depths, followed by an evident analogous increase in spring and summer (with some exceptions) mass flux. Such an interannual change in flux patterns could be explained by the reinforcement of processes which produce and/or transfer particulate matter in the area.

A plausible reason for the increase of fluxes from 2006 to 2010 could be related to the general circulation patterns of the study site, which exhibit strong interannual variability. During mid-late 1990s the large scale anticyclonic circulation observed during the 1980s and early 1990s was confined in the southern part and replaced by a cyclonic circulation in the northern Ionian (Borzelli et al., 2009; Gačić et al., 2011; Larnicol et al., 2002). In the years following 2006, the salinity and nutrient changes in the south Adriatic suggest that the Ionian circulation was changed back into anticyclonic (Civitarese et al., 2010). This latter circulation regime causes the upwelling of the nutricline in the periphery of the anticyclonic gyre and the weakening or even the absence of the Pelops gyre. The NESTOR site is obviously found at the edge of this anticyclone as revealed from the recurrent shoaling of the isohalines recorded in the nearby observational buoy of the Poseidon system (Fig. 9). Furthermore, the remarkable enhancement of the fluxes from 2008 onwards seems to be directly dependent on the intensity of the intrusion in the upper layer of high salinity intermediate waters of Levantine/Cretan origin. The upward movement of these intermediate waters could favor upwelling of nutrients and enrichment of the upper layer, thus triggering surface productivity and the enhancement of downward particle fluxes. In respect to this hypothesis, the increased contribution of all biogenic (OC, carbonate, opal) constituents in late spring/summer of 2008 and 2009, suggests an effective nutrient fueling of the upper layer created by the dynamic conditions prevailing in the vicinity of NESTOR site.

BGD
10, 591–641, 2013

The large scale processes and changes affecting the Ionian Sea is considered to play a crucial role in the production of phytoplanktonic biomass (D'Ortenzio et al., 2003) and may control the biogeochemical functioning of the Ionian Sea.

5.4 Organic carbon export

Depth profiles of sinking particle fluxes in the ocean are characterized by rapid attenuation of POC fluxes in the mesopelagic zone between the base of the euphotic zone (∼ 100–200 m) and roughly 1000 m, below which < 10 % of the export flux is detectable (Buesseler, 1998). The pronounced gradient with depth demonstrates that length scales of remineralization increase with depth. Explanations commonly offered for this behavior include the existence of different reactivity classes of organic matter that attenuate sequentially with depth or time along with the more extensive heterotrophic processing of organic matter in the biologically more active upper water column (Berner, 1980; Wakeham and Lee, 1993), and the "ballast" hypothesis, claiming that organic matter is better preserved in sinking particles, due to increased aggregate density and sinking velocity and/or via protection, when ballast minerals are present (Armstrong et al., 2002; Francois et al., 2002; Klaas and Archer, 2002). Since Suess (1980), there have been many attempts to describe the change in POC flux with depth using sediment trap measurements and employing empirical relationships (e.g. Buesseler and Boyd, 2009 and references therein; Francois et al., 2002; Honda et al., 1997; Martin et al., 1987). The most commonly used is the Martin curve (Martin et al., 1987), expressed as:

$$F_z = F_{100}\left(z/100\right)^b \tag{1}$$

where, F_z is the POC flux at depth z (m), F_{100} is the POC flux at 100 m, and b is a unitless parameter determining the degree of flux attenuation with depth (F_{100} = 50.4 mg C m^{-2} d^{-1}, and $b = -0.858$ in the original equation). The exponent b is not a constant factor (Francois et al., 2002; Lutz et al., 2002) and it is controlled by several

BGD
10, 591–641, 2013

biological and physical processes, i.e. zooplankton swimming and excretion at depth (Bishop et al., 1986; Bishop, 1989), variability of the mixed layer depth (Fischer et al., 1996), plankton community structure (Boyd and Newton, 1995).

In order to estimate carbon export ratios in the oligotrophic Ionian Sea, we used primary production values from the literature, organic carbon fluxes obtained by the 5 NESTOR sediment traps and the f-ratio defined as the proportion of primary production exported from the euphotic zone (Eppley and Peterson, 1979).

Primary production values are derived either from satellite imagery (Antoine and Morel, 1995; Bosc et al., 2004; Bricaud et al., 2002; Colella et al., 2004) or from direct measurements (Bianchi et al., 1999; Moutin and Raimbault, 2002). For the eastern Mediterranean basin, Bricaud et al. (2002) reported primary production between 375 and 501 $mg\,C\,m^{-2}\,d^{-1}$, whereas for the North Ionian, Bosc et al. (2004) reported values between 318 and 356 $mg\,C\,m^{-2}\,d^{-1}$. Colella et al. (2004) using satellite data estimated a mean primary production of 241 $mg\,C\,m^{-2}\,d^{-1}$ for the Ionian Sea, which is slightly lower than the 285 $mg\,C\,m^{-2}\,d^{-1}$ given by Antoine and Morel (1995) for the entire Ionian basin. Recently, Taillandier et al. (2012), reported 323 $mg\,C\,m^{-2}\,d^{-1}$ (SeaWiFS for the period 1998–2001) total primary production for the Eastern Mediterranean Sea. Estimates of primary production measured by ^{14}C in the north Ionian were 169 $mg\,C\,m^{-2}\,d^{-1}$ (Bianchi et al., 1999), and between 255 and 325 $mg\,C\,m^{-2}\,d^{-1}$ during May–June 1996 (Moutin and Raimbault, 2002). For the calculations, the daily annual mean of 241 $mg\,C\,m^{-2}\,d^{-1}$ (Colella et al., 2004) is used because: (1) this value refers to the Ionian basin rather than the entire Eastern Mediterranean; and (2) primary production estimates based on direct measurements in the Ionian Sea are intermittent. Using the primary production reported by Colella et al. (2004) and the f-ratio of 0.15 given by Laws et al. (2000) for oligotrophic areas, an organic carbon flux of 36 $mg\,C\,m^{-2}\,d^{-1}$ at 100 m depth was calculated. The latter value and OC flux data as calculated in our sediment trap experiment were used to obtain the exponent b of Martin's equation, providing $b = -1.07$. Francois et al. (2002) reported b values ranging between −2.01 and −0.59, from numerous sites distributed ocean-wide. Sanchez-Vidal et al. (2005)

determined the exponent *b* for data of the Alboran Sea and give a value of −0.753, while Zuniga et al. (2007) for the Algero-Balearic basin provide a value of −0.918. Our *b* exponent is more negative than those previously reported for the western Mediterranean, and probably indicates greater particulate organic carbon flux attenuation in the upper several hundred meters (Buesseler and Boyd, 2009).

In Table 4, we compared export ratios at the collecting depths and at 100 m with the estimations obtained using the empirical models of Betzer et al. (1984), Suess (1980), and Pace et al. (1987). The organic carbon fluxes, and thus the export ratios, were always underestimated, with the higher deviation to be observed at 100 m depth, decreasing towards the deeper waters. The export ratios estimated from the sediment trap data are also low, compared to those reported for other oceanic areas (Honda, 2003). The worldwide estimation of the fraction of POC transported to the global ocean at depths > 1500 m ranges from 0.10 to 8.8 % (average 1.1 %) of surface primary production, and from 0.28 to 30 % (average 5.7 %) of export from the base of the euphotic zone (Lutz et al., 2002). Our values below the 1500 m depth are between 0.46 and 0.72 %, i.e. lower than the global average of 1.1 %, whereas the available organic carbon to export below the euphotic zone (8.6 % of photosynthetically produced organic carbon) is higher than the global average of 5.5 % (Lutz et al., 2002) Zuniga et al. (2007) give export ratios in the Algero-Balearic basin (Western Mediterranean) higher (2.42–0.70 %), but comparable to our values. In the Alboran Sea (SW Mediterranean), Sanchez-Vidal et al. (2005) report much higher values (5.74–1.79 %). Moutin and Raimbault (2002), using free drifting sediment traps in the Ionian Sea, reported export ratios at 100 m between 2.8 and 3.4 % (May–June 1996), and Lepore at al. (2009) reported an export ratio of 6.1 % in the south Aegean (Cretan Sea), possibly during early spring bloom; those values are lower, but comparable to our estimates. Boldrin et al. (2002) provided for the north Ionian export ratios of 3.9 % and 0.8 %, at 150 m and 2250 m depth, respectively, values relatively similar to our export ratios. The export ratio of ~ 8 % at 100 m (Table 4), reveals that ~ 92 % of the organic carbon produced by photosynthetic processes has been respired back to inorganic carbon or released as

BGD
10, 591–641, 2013

dissolved organic carbon in the first 100 m of the water column (Sanchez-Vidal et al., 2005). Finally, only a small portion of primary production reach at 4300 m depth, ranging between 0.15 and 1.87 %, or 0.13 and 1.64 $\mathrm{g\,C\,m^{-2}\,yr^{-1}}$.

5.5 Relation between organic matter and mineral ballast fluxes

Previous studies have shown that the fluxes of ballast minerals (calcium carbonate, opal, and lithogenic material) and the organic carbon fluxes are closely correlated in the bathypelagic zones of the ocean, leading to a hypothesis that organic carbon export is determined by the presence of ballast minerals within settling aggregates (Armstrong et al., 2002; Francois et al., 2002; Klaas and Archer, 2002). Klaas and Archer (2002) observed that ~ 83 % of the global particulate organic carbon (POC) fluxes were associated with carbonate, and suggested that carbonate is a more efficient ballast mineral as compared to opal and terrigenous material. However, De La Rocha et al. (2008) found no evidence supporting calcium carbonate as a better carrier of organic matter than opal. Still, Klaas and Archer (2002) and Passow (2004) proposed the "glue hypothesis" to suggest that the OC : ballast relationship was due to the physical scavenging of minerals by sinking OC. According to this, incorporation of inorganic minerals might increase the sinking rates of the OC-rich marine snow material, but would not initially ballast the particles sufficiently to drive them sink. Previous investigations demonstrated that organic-rich "gels" are abundant and important components of aggregates throughout the water column of the oceans (Engel et al., 2004; Gogou et al., 2010; Passow et al., 2001; Verdugo et al., 2004). Riley et al. (2012) recently presented a model that considers suspended particles, slow sinking particles that are subject to remineralization in the water column, and fast sinking particles that may be subject to ballasting.

Potential relationships between OC, mass flux of sinking particles and ballast minerals are examined in Fig. 12a–c. Ballast mineral fluxes, they all exhibit very good correlations with OC fluxes ($r^2 = 0.86$ for all correlations of OC vs. ballast minerals). Lee et al. (2009) noticed that during the MedFlux experiment at the Dyfamed site (Western

BGD
10, 591–641, 2013

Mediterranean) fluxes were decoupled from satellite Chl *a* values, and they proposed that the triggering for causing particle aggregation could be a "catalyst", namely the ballasted plankton and lithogenic particles during the high productive and dust-influenced periods, respectively. The oligotrophic character of our study site, with low OC contents for particles reaching higher depths, pinpoints to a similar mechanism to that described by Lee et al. (2009) with organic matter to be related though "glue" or ballasting processes to different types of available inorganic matrices (e.g. carbonate, opal and lithogenics) during carbonate- or silicious-species blooming and during episodic dust input events.

In our study, a power function gave the best fit for organic carbon versus mass flux (Fig. 12d). The OC content (%) increases towards the periods characterized by lower particulate export rates. Given that much of the mass flux is not represented by OC, but is due to ballast minerals, these results suggest that the OC/ballast ratio is higher for more slowly settling material, as reported by Lee et al. (2009). This can also be seen in more temporal detail in measurements of OC, carbonate, opal and lithogenic fluxes, showing higher relative contributions of organic matter and reduced contributions of mineral ballast in the upper trap during the low mass flux periods, while the opposite trend is apparent for high flux periods (Figs. 5 to 8).

Acknowledgements. This work was supported by the HERMIONE FP7-DG-Environment, KM3NET/FP6-DG-Environment and MEDECOS (Marin-ERA, FP6) EU Projects and the Greek General Secretariat of Research and Technology. We gratefully acknowledge the officers and crew of the R/V *Aegaeo* for their invaluable assistance during the numerous mooring deployments and recoveries sometimes under rough weather conditions. We are also thankful for their technical assistance onboard to Panagiotis Renieris and Thanasis Morfis.

BGD
10, 591–641, 2013

References

Aït-Ameur, N. and Goyet, C.: Distribution and transport of natural and anthropogenic CO_2 in the Gulf of Cádiz, Deep-Sea Res. Pt. II, 53, 1329–1343, doi:10.1016/j.dsr2.2006.04.003, 2006.

Álvarez, M., Pérez, F., Shoosmith, D. R., and Bryden, H. L.: Unaccounted role of Mediterranean water in the drawdown of anthropogenic carbon, J. Geophys. Res.-Oceans, 110, 1–18, doi:10.1029/2004jc002633, 2005.

Antoine, D., Morel, A., and Andre, J. M.: Algal pigment distribution and primary production in the eastern Mediterranean as derived from coastal zone color scanner observations, J. Geophys. Res., 100, 16193–16209, 1995.

Armstrong, R. A., Lee, C., Hedges, J. I., Honjo, S., and Wakeham, S. G.: A new, mechanistic model for organic carbon fluxes in the ocean based on the quantitative association of POC with ballast minerals, Deep-Sea Res. Pt. II, 49, 219–236, doi:10.1016/s0967-0645(01)00101-1, 2002.

Berner R. A.: Early Diagenesis, a Theoretical Approach, Princeton University Press, Princeton, NJ, 241 pp., 1980.

Betzer, P. R., Showers, W. J., Laws, E. A., Winn, C. D., DiTullio, G. R., and Kroopnick, P. M.: Primary productivity and particle fluxes on a transect of the equator at 153° W in the Pacific Ocean, Deep Sea Res. A, 31, 1–11, 1984.

Bianchi, F., Boldrin, A., Civitarese, G., Del Negro, P., Giordani, P., Malaguti, A., Socal, G., Rabitti, S., and Turchetto, M. M.: Biogenic particulate matter and primary productivity in the Southern Adriatic and Northern Ionian seas, 4th MTP-Workshop MATER, Perpignan (France), Abstracts Volume, Les Presses Littéraires, Saint-Esteve, 120–121, 1999.

Bishop J. K. B.: Regional extremes in particulate matter composition and flux: effects on the chemistry of the ocean interior, In: Productivity of the Ocean: Present and Past, edited by: Berger, W. H., Smetacek, V. S., and Wefer, G., John Willey and Sons Ltd., 117–137, 1989.

Bishop, J. K. B., Stepien, J. C., and Wiebe, P. H.: Particulate matter distributions, chemistry and flux in the panama basin: response to environment forcing, Prog. Oceanogr., 17, 1–59, 1986.

Boldrin, A., Miserocchi, S., Rabitti, S., Turchetto, M. M., Balboni, V., and Socal, G.: Particulate matter in the southern Adriatic and Ionian Sea: characterisation and downward fluxes, J. Mar. Syst., 33–34, 389–410, 2002.

BGD
10, 591–641, 2013

Downward fluxes of sinking particulate matter in the deep Ionian Sea

S. Stavrakakis et al.

Borzelli, G. L. E., Gačič, M., Cardin, V., and Civitarese, G.: Eastern mediterranean transient and reversal of the Ionian Sea circulation, Geophys. Res. Lett., 36, L15108, doi:10.1029/2009gl039261, 2009.
Bosc, E., Bricaud, A., and Antoine, D.: Seasonal and interannual variability in algal biomass and primary production in the Mediterranean Sea, as derived from 4 yr of SeaWiFS observations, Global Biogeochem. Cy., 18, GB1005, doi:10.1029/2003GB002034, 2004.
Boyd, P. and Newton, P.: Evidence of the potential influence of planktonic community structure on the interannual variability of particulate organic carbon flux, Deep-Sea Res. Pt. I, 42, 619–639, doi:10.1016/0967-0637(95)00017-z, 1995.
Bricaud, A., Bosc, E., and Antoine, D.: Algal biomass and sea surface temperature in the Mediterranean Basin Intercomparison of data from various satellite sensors, and implications for primary production estimates, Remote Sens. Environ., 81, 163–178, doi:10.1016/s0034-4257(01)00335-2, 2002.
Broecker W. S. and Peng T. H.: Tracers in the Sea, Lamont-Doherty Geological Observatory, Palisades, NY, 1982.
Buesseler, K. O.: The decoupling of production and particulate export in the surface ocean, Global Biogeochem. Cy., 12, 297–310, 1998.
Buesseler, K. O. and Boyd, P. W.: Shedding light on processes that control particle export and flux attenuation in the twilight zone of the open ocean, Limnol. Oceanogr., 54, 1210–1232, doi:10.1029/2004GB002390, 2009.
Buesseler, K. O., Lamborg, C. H., Boyd, P. W., Lam, P. J., Trull, T. W., Bidigare, R. R., Bishop, J. K. B., Casciotti, K. L., Dehairs, F., Elskens, M., Honda, M., Karl, D. M., Siegel, D. A., Silver, M. W., Steinberg, D. K., Valdes, J., Van Mooy, B., and Wilson, S.: Revisiting carbon flux through the ocean's twilight zone, Science, 316, 567–570, doi:10.1126/science.1137959, 2007.
Canals, M., Puig, P., De Madron, X. D., Heussner, S., Palanques, A., and Fabres, J.: Flushing submarine canyons, Nature, 444, 354–357, doi:10.1038/nature05271, 2006.
Casotti, R., Landolfi, A., Brunet, C., D'Ortenzio, F., Mangoni, O., Ribera d'Alcala, M., and Denis, M.: Composition and dynamics of the phytoplankton of the Ionian Sea (eastern Mediterranean), J. Geophys. Res., 108, 8116, doi:10.1029/2002JC001541, 2003.
Civitarese, G., Gačić, M., Lipizer, M., and Eusebi Borzelli, G. L.: On the impact of the Bimodal Oscillating System (BiOS) on the biogeochemistry and biology of the Adriatic and Io-

BGD
10, 591–641, 2013

nian Seas (Eastern Mediterranean), Biogeosciences, 7, 3987–3997, doi:10.5194/bg-7-3987-2010, 2010.
Colella, S., D'Ortenzio, F., Marullo, S., Santoleri, R., Ragni, M., and Ribera d'Alcala, M.: Primary production variability in the Mediterranean Sea from SeaWiFS data, Proc. SPIE 5233, Remote Sensing of the Ocean and Sea Ice 2003, 371, doi:10.1117/12.516791, 2004.
Conte, M. H., Ralph, N., and Ross, E. H.: Seasonal and interannual variability in deep ocean particle fluxes at the Oceanic Flux Program (OFP)/Bermuda Atlantic Time Series (BATS) site in the western Sargasso Sea near Bermuda, Deep-Sea Res. Pt. II, 48, 1471–1505, 2001.
Crombet, Y., Leblanc, K., Quéguiner, B., Moutin, T., Rimmelin, P., Ras, J., Claustre, H., Leblond, N., Oriol, L., and Pujo-Pay, M.: Deep silicon maxima in the stratified oligotrophic Mediterranean Sea, Biogeosciences, 8, 459–475, doi:10.5194/bg-8-459-2011, 2011.
Cutter, G. A. and Radford-Knoery, J.: Determination of carbon, nitrogen, sulfur and inorganic sulfur species in marine particles, in: Marine Particles: Analysis and Characterization, edited by: Hurd, D. C. and Spencer, D. W., American Geophysical Union, Geophys. Monogr., 63, 57–63, 1991.
De Lazzari, A., Boldrin, A., Rabitti, S., and Turchetto, M. M.: Variability and downward fluxes of particulate matter in the Otranto Strait area, J. Mar. Syst., 20, 399–413, doi:10.1016/s0924-7963(98)00076-1, 1999.
De La Rocha, C. L., Nowald, N., and Passow U. Interactions between diatom aggregates, minerals, particulate organic carbon, and dissolved organic matter: further implications for the ballast hypothesis, Global Biogeochem. Cy., 22, GB4005, doi:10.1029/2007GB003156, 2008
D'Ortenzio, F. and Ribera d'Alcalà, M.: On the trophic regimes of the Mediterranean Sea: a satellite analysis, Biogeosciences, 6, 139–148, doi:10.5194/bg-6-139-2009, 2009.
D'Ortenzio, F., Ragni, M., Marullo, S., and Ribera d'Alcala, M.: Did biological activity in the Ionian Sea change after the Eastern Mediterranean Transient? Results from the analysis of remote sensing observations, J. Geophys. Res., 108, 8113, doi:10.1029/2002JC001556, 2003.
Engel, A., Thoms, S., Riebesell, U., Rochelle-Newall, E., and Zondervan, I.: Polysaccharide aggregation as a potential sink of marine dissolved organic carbon, Nature, 428, 929–932, 2004.
Eppley, R. W., and Peterson, B. J.: Particulate organic matter flux and planktonic new production in the deep ocean, Nature, 282, 677–680, doi:10.1038/282677a0, 1979.

Fabres, J., Tesi, T., Velez, J., Batista, F., Lee, C., Calafat, A., Heussner, S., Palanques, A., and Miserocchi, S.: Seasonal and event-controlled export of organic matter from the shelf towards the Gulf of Lions continental slope, Cont. Shelf Res., 28, 1971–1983, doi:10.1016/j.csr.2008.04.010, 2008.

Fischer, G., Donner, B., Ratmeyer, V., Davenport, R., and Wefer, G.: Distinct year-to-year particle flux variations off Cape Blanc during 1988–1991: relation to δ^{18}O-deduced sea-surface temperatures and trade winds, J. Mar. Res., 54, 73–98, 1996.

Francois, R., Honjo, S., Krishfield, R., and Manganini, S.: Factors controlling the flux of organic carbon to the bathypelagic zone of the ocean, Global Biogeochem. Cy., 16, 34–31, 2002.

Gačić, M., Civitarese, G., Eusebi Borzelli, G. L., Kovačević, V., Poulain, P.-M., Theocharis, A., Menna, M., Catucci, A., and Zarokanellos, N.: On the relationship between the decadal oscillations of the northern Ionian Sea and the salinity distributions in the eastern Mediterranean, J. Geophys. Res., 116, C12002, doi:10.1029/2011JC007280, 2011.

Gogou, A. and Repeta, D. J.: Particulate-dissolved transformations as a sink for semi-labile dissolved organic matter: chemical characterization of high molecular weight dissolved and surface-active organic matter in seawater and in diatom cultures, Mar. Chem., 121, 215–223, 2010.

Gogou, A., Sanchez-Vidal, A., Stavrakakis, S., Durrieu de Madron, X., Calafat, A., Stabholz, M., Psarra, S., Canals, M., Heussner, S., Stavrakaki, I., and Papathanassiou, V.: Carbon flux to the deep in three open sites of the Southern European seas, submitted to Journal of Marine Systems, 2012.

Guerzoni, S., Chester, R., Dulac, F., Herut, B., Loÿe-Pilot, M. D., Measures, C., Migon, C., Molinaroli, E., Moulin, C., Rossini, P., Saydam, C., Soudine, A., and Ziveri, P.: The role of atmospheric deposition in the biogeochemistry of the Mediterranean Sea, Prog. Oceanogr., 44, 147–190, doi:10.1016/s0079-6611(99)00024-5, 1999.

Haake, B., Ittekkot, V., Rixen, T., Ramaswamy, V., Nair, R. R., and Curry, W. B.: Seasonality and interannual variability of particle fluxes to the deep Arabian sea, Deep-Sea Res. Pt. I, 40, 1323–1344, 1993.

Herut, B., Collier, R., and Krom, M. D.: The role of dust in supplying nitrogen and phosphorus to the Southeast Mediterranean, Limnol. Oceanogr., 47, 870–878, 2002.

Heussner, S., Ratti, C., and Carbonne, J.: The PPS 3 time-series sediment trap and the trap sample processing techniques used during the ECOMARGE experiment, Cont. Shelf Res., 10, 943–958, 1990.

Heussner, S., Durrieu de Madron, X., Calafat, A., Canals, M., Carbonne, J., Delsaut, N., and Saragoni, G.: Spatial and temporal variability of downward particle fluxes on a continental slope: lessons from an 8-yr experiment in the Gulf of Lions (NW Mediterranean), Mar. Geol., 234, 63–92, doi:10.1016/j.margeo.2006.09.003, 2006.

Honda, M. C., Kusakabe, M., Nakabayashi, S., Manoanini, S. J., and Honjo, S.: Change in $p\mathrm{CO_2}$ through biological activity in the marginal seas of the western North Pacific: the efficiency of the biological pump estimated by a sediment trap experiment, J. Oceanogr., 53, 645–662, 1997.

Honda, M. C.: Biological pump in Northwestern North Pacific, J. Oceanogr., 59, 671–684, 2003

Honjo, S., Manganini, S. J., Krishfield, R. A., and Francois, R.: Particulate organic carbon fluxes to the ocean interior and factors controlling the biological pump: a synthesis of global sediment trap programs since 1983, Prog. Oceanogr., 76, 217–285, 2008.

Ignatiades, L., Gotsis-Skretas, O., Pagou, K., and Krasakopoulou, E.: Diversification of phytoplankton community structure and related parameters along a large-scale longitudinal east-west transect of the Mediterranean Sea, J. Plankton Res., 31, 411–428, doi:10.1093/plankt/fbn124, 2009.

Ittekkot, V., Haake, B., Bartsch, M., Nair, R. R., and Ramaswamy, V.: Organic carbon removal in the sea: the continental connection, in: Upwelling Systems: Evolution Since the Early Miocene, edited by: Prell, C. P. and Emeis, K. C., Geol. Society Spec. Publ. No. 64, 167–176, 1992.

Karageorgis, A. P.: Suspended particulate matter distribution at the NESTOR site, using optical methods and bottle data, KM3NeT Collaboration Meeting 16–18 April 2007, Pylos, Greece, 2007.

Karageorgis, A. P., Gardner, W. D., Georgopoulos, D., Mishonov, A. V., Krasakopoulou, E., and Anagnostou, C.: Particle dynamics in the Eastern Mediterranean Sea: a synthesis based on light transmission, PMC, and POC archives (1991–2001), Deep-Sea Res. Pt. I, 55, 177–202, doi:10.1016/j.dsr.2007.11.002, 2008.

Karageorgis, A. P., Georgopoulos, D., Kanellopoulos, T. D., Mikkelsen, O. A., Pagou, K., Kontoyiannis, H., Pavlidou, A., and Anagnostou, C.: Spatial and seasonal variability of particulate matter optical and size properties in the Eastern Mediterranean Sea, J. Mar. Syst., 105–108, 123–134, doi:10.1016/j.jmarsys.2012.07.003, 2012.

BGD
10, 591–641, 2013

Downward fluxes of sinking particulate matter in the deep Ionian Sea

S. Stavrakakis et al.

Karl, D. M., Christian, J. R., Dore, J. E., Hebel, D. V., Letelier, R. M., Tupas, L. M., and Winn, C. D.: Seasonal and interannual variability in primary production and particle flux at station ALOHA, Deep-Sea Res. Pt. II, 43, 539–568, 1996.

Karl, D. M., Dore, J. E., Lukas, R., Michaels, A. F., Bates, N. R., and Knap, A.: Building the long-term picture: the US JGOFS time-series programs, Oceanography, 14, 6–17, 2001.

Kerhervé, P., Heussner, S., Charrière, B., Stavrakakis, S., Ferrand, J. L., Monaco, A., and Delsaut, N.: Biogeochemistry and dynamics of settling particle fluxes at the Antikythira Strait (Eastern Mediterranean), Prog. Oceanogr., 44, 651–675, doi:10.1016/s0079-6611(99)00040-3, 1999.

Klaas, C. and Archer, D. E.: Association of sinking organic matter with various types of mineral ballast in the deep sea: implications for the rain ratio, Global Biogeochem. Cy., 16, 63–61, doi:10.1029/2001GB001722, 2002.

Klein, B., Roether, W., Manca, B. B., Bregant, D., Beitzel, V., Kovacevic, V., and Luchetta, A.: The large deep water transient in the eastern Mediterranean, Deep Sea Res. II, 46, 371–414, 1999.

Km3NeT Collaboration: Report on evaluation of existing water, oceanographic, biological and geological data from candidate sites, Km3NeT Report, WP5, Deliverable 5.1, 2007.

Knauer, G. A., Karl, D. M., Martin, J. H., and Hunter, C. N.: In situ effects of selected preservatives on total carbon, nitrogen and metals collected in sediment traps, J. Mar. Res., 42, 445–462, 1984.

Kontoyiannis, H. and Lykoysis, V.: Was the East Mediterranean deep thermohaline cell weakening during 2006–2009?, Nucl. Instrum. Meth. A, 626–627, 91–93, 2011.

Kouvarakis, G., Mihalopoulos, N., Tselepides, A., and Stavrakakis, S.: On the importance of atmospheric inputs of inorganic nitrogen species on the productivity of the Eastern Mediterranean sea, Global Biogeochem. Cy., 15, 805–817, doi:10.1029/2001gb001399, 2001.

Krasakopoulou, E., Souvermezoglou, E., and Goyet, C.: Anthropogenic CO_2 fluxes in the Otranto Strait (E. Mediterranean) in February 1995, Deep-Sea Res. Pt. I, 58, 1103–1114, doi:10.1016/j.dsr.2011.08.008, 2011.

Krom, M. D., Kress, N., Brenner, S., and Gordon, L. I.: Phosphorus limitation of primary productivity in the eastern Mediterranean Sea, Limnol. Oceanogr., 36, 424–432, 1991.

Lampitt, R. S. and Antia, A. N.: Particle flux in deep seas: regional characteristics and temporal variability, Deep-Sea Res. Pt. I, 44, 1377–1403, doi:10.1016/s0967-0637(97)00020-4, 1997.

BGD
10, 591–641, 2013

Larnicol, G., Ayoub, N., and Le Traon, P. Y.: Major changes in Mediterranean Sea level variability from 7 yr of TOPEX/Poseidon and ERS-1/2 data, J. Mar. Syst., 33–34, 63–89, 2002.
Laws, E. A., Falkowski, P. G., Smith Jr., W. O., Ducklow, H., and McCarthy, J. J.: Temperature effects on export production in the open ocean, Global Biogeochem. Cy., 14, 1231–1246, doi:10.1029/1999gb001229, 2000.
Lee, C., Peterson, M. L., Wakeham, S. G., Armstrong, R. A., Cochran, J. K., Miquel, J. C., Fowler, S. W., Hirschberg, D., Beck, A., and Xue, J.: Particulate organic matter and ballast fluxes measured using time-series and settling velocity sediment traps in the northwestern Mediterranean Sea, Deep-Sea Res. Pt. II, 56, 1420–1436, doi:10.1016/j.dsr2.2008.11.029, 2009.
Lepore, K., Moran, S. B., Burd, A. B., Jackson, G. A., Smith, J. N., Kelly, R. P., Kaberi, H., Stavrakakis, S., and Assimakopoulou, G.: Sediment trap and in-situ pump size-fractionated POC/^{234}Th ratios in the Mediterranean Sea and Northwest Atlantic: implications for POC export, Deep-Sea Res. Pt. I, 56, 599–613, doi:10.1016/j.dsr.2008.11.004, 2009.
López-Sandoval, D. C., Fernández, A., and Marañón, E.: Dissolved and particulate primary production along a longitudinal gradient in the Mediterranean Sea, Biogeosciences, 8, 815–825, doi:10.5194/bg-8-815-2011, 2011.
Loÿe-Pilot, M. D., Martin, J. M., and Morelli, J.: Atmospheric input of inorganic nitrogen to the Western Mediterranean, Biogeochemistry, 9, 117–134, doi:10.1007/bf00692168, 1990.
Lutz, M., Dunbar, R., and Caldeira, K.: Regional variability in the vertical flux of particulate organic carbon in the ocean interior, Global Biogeochem. Cy., 16, 1037, doi:10.1029/2000GB001383, 2002.
Malanotte-Rizzoli, P., Manca, B., Ribera D'Alcala, M., Theocharis, A., Bergamasco, A., Bregant, D., Budillon, G., Civitarese, G., Georgopoulos, D., Michelato, A., Sansone, E., Scarazzato, P., and Souvermezoglou, E.: A synthesis of the Ionian Sea hydrography, circulation and water mass pathways during POEM-Phase I, Prog. Oceanogr., 39, 153–204, 1997.
Malanotte-Rizzoli, P., Manca, B. B., Ribera d'Alcala, M., Theocharis, A., Brenner, S., Budillon, G., and Ozsoy, E.: The Eastern Mediterranean in the 80s and in the 90s: the big transition in the intermediate and deep circulations, Dynam. Atmos. Oceans, 29, 365–395, doi:10.1016/S0377-0265(99)00011-1, 1999.
Malinverno, E., Triantaphyllou, M. V., Stavrakakis, S., Ziveri, P., and Lykousis, V.: Seasonal and spatial variability of coccolithophore export production at the South-

Western margin of Crete (Eastern Mediterranean), Mar. Micropaleontol., 71, 131–147, doi:10.1016/j.marmicro.2009.02.002, 2009.
Manca, B. B., Budillon, G., Scarazzato, P., and Ursella, L.: Evolution of dynamics in the eastern Mediterranean affecting water mass structures and properties in the Ionian and Adriatic Seas, J. Geophys. Res.-Oceans, 108, PBE 3-1-3-19, 10.1029/ 2002JC001645, 2003.
Markaki, Z., Oikonomou, K., Kocak, M., Kouvarakis, G., Chaniotaki, A., Kubilay, N., and Mihalopoulos, N.: Atmospheric deposition of inorganic phosphorus in the Levantine Basin, eastern Mediterranean: spatial and temporal variability and its role in seawater productivity, Limnol. Oceanogr., 48, 1557–1568, doi:10.1029/2000JD000291, 2003.
Martin, J. H., Knauer, G. A., Karl, D. M., and Broenkow, W. W.: VERTEX: carbon cycling in the northeast Pacific, Deep Sea Res. Pt. A, 34, 267–285, 1987.
Martin, J., Miquel, J. C., and Khripounoff, A.: Impact of open sea deep convection on sediment remobilization in the western Mediterranean, Geophys. Res. Lett., 37, L13604, doi:10.1029/2010GL043704, 2010.
Mazzocchi, M. G., Nervegna, D., D'Elia, G., Di Capua, I., Aguzzi, L., and Boldrin, A.: Spring mesozooplankton communities in the epipelagic Ionian Sea in relation to the Eastern Mediterranean Transient, J. Geophys. Res., 108, 8114, doi:10.1029/2002JC001640, 2003.
Meador, T. B., Gogou, A., Spyres, G., Herndl, G. J., Krasakopoulou, E., Psarra, S., Yokokawa, T., De Corte, D., Zervakis, V., Repeta, D. J.: Biogeochemical relationships between ultrafiltered dissolved organic matter and picoplankton activity in the Eastern Mediterranean Sea, Deep-Sea Res. Pt. II, 57, 1460–1477, 2010.
Miquel, J. C., Martín, J., Gasser, B., Rodriguez-y-Baena, A., Toubal, T., and Fowler, S. W.: Dynamics of particle flux and carbon export in the northwestern Mediterranean Sea: a two decade time-series study at the DYFAMED site, Prog. Oceanogr., 91, 461–481, doi:10.1016/j.pocean.2011.07.018, 2011.
Monaco, A., Durrieu de Madron, X., Radakovitch, O., Heussner, S., and Carbonne, J.: Origin and variability of downward biogeochemical fluxes on the Rhone continental margin (NW Mediterranean), Deep-Sea Res. Pt. I, 46, 1483–1511, doi:10.1016/s0967-0637(99)00014-x, 1999.
Mortlock, R. A. and Froelich, P. N.: A simple method for the rapid determination of biogenic opal in pelagic marine sediments, Deep-Sea Res., 36, 1415–1426, 1989.

BGD
10, 591–641, 2013
Downward fluxes of sinking particulate matter in the deep Ionian Sea
S. Stavrakakis et al.

Moutin, T. and Raimbault, P.: Primary production, carbon export and nutrients availability in western and eastern Mediterranean Sea in early summer 1996 (MINOS cruise), J. Mar. Syst., 33–34, 273–288, 2002.

Nieuwenhuize, J., Maas, Y. E. M., and Middelburg, J. J.: Rapid analysis of organic carbon and nitrogen in particulate materials, Mar. Chem., 45, 217–224, 1994.

Nittis, K., Pinardi, N., and Lascaratos, A.: Characteristics of the summer 1987 flow field in the Ionian Sea, J. Geophys. Res., 98, 10171–10184, 1993.

Pace, M. L., Knauer, G. A., Karl, D. M., and Martin, J. H.: Primary production, new production and vertical flux in the eastern Pacific Ocean, Nature, 325, 803–804, 1987.

Pasqual, C., Sanchez-Vidal, A., Zúñiga, D., Calafat, A., Canals, M., Durrieu de Madron, X., Puig, P., Heussner, S., Palanques, A., and Delsaut, N.: Flux and composition of settling particles across the continental margin of the Gulf of Lion: the role of dense shelf water cascading, Biogeosciences, 7, 217–231, doi:10.5194/bg-7-217-2010, 2010.

Passow, U.: Switching perspectives: do mineral fluxes determine particulate organic carbon fluxes or vice versa?, Geochem. Geophys. Geosyst., 5, doi:10.1029/2003gc000670, 2004.

Passow, U., Shipe, R. F., Murray, A., Pak, D. K., Brzezinski, M. A., and Alldredge, A. L.: Origin of transparent exopolymer particles (TEP) and their role in the sedimentation of particulate matter, Cont. Shelf Res., 21, 327–346, 2001.

Patara, L., Pinardi, N., Corselli, C., Malinverno, E., Tonani, M., Santoleri, R., and Masina, S.: Particle fluxes in the deep Eastern Mediterranean basins: the role of ocean vertical velocities, Biogeosciences, 6, 333–348, doi:10.5194/bg-6-333-2009, 2009.

Polymeris, G. S., Kitis, G., Liolios, A. K., Sakalis, A., Zioutas, K., Anassontzis, E. G., and Tsirliganis, N. C.: Luminescence dating of the top of a deep water core from the NESTOR site near the Hellenic Trench, east Mediterranean Sea, Quat. Geochronol., 4, 68–81, 2009.

Rabitti, S., Bianchi, F., Boldrin, A., Da Ros, L., Socal, G., and Totti, C.: Particulate matter and phytoplankton in the Ionian Sea, Oceanol. Acta, 17, 297–307, 1994.

Ridame, C. and Guieu, C.: Saharan input of phosphate to the oligotrophic water of the open western Mediterranean sea, Limnol. Oceanogr., 47, 856–869, 2002.

Riley, J. S., Sanders, R., Marsay, C., Le Moigne, F. A. C., Achterberg, E. P., and Poulton, A. J.: The relative contribution of fast and slow sinking particles to ocean carbon export, Global Biogeochemical Cycles, 26, GB1026, doi:10.1029/2011GB004085, 2012.

Sabine, C. L. and Tanhua, T.: Estimation of anthropogenic CO_2 inventories in the ocean, Annu. Rev. Mar. Sci., 2, 175–198, doi:10.1146/annurev-marine-120308-080947, 2010.

Sanchez-Vidal, A., Calafat, A., Canals, M., Frigola, J., and Fabres, J.: Particle fluxes and organic carbon balance across the Eastern Alboran Sea (SW Mediterranean Sea), Cont. Shelf Res., 25, 609–628, doi:10.1016/j.csr.2004.11.004, 2005.

Schneider, A., Tanhua, T., Krtzinger, A., and Wallace, D. W. R.: High anthropogenic carbon content in the eastern Mediterranean, J. Geophys. Res., 115, C12050, doi:10.1029/2010JC006171, 2010.

Siokou-Frangou, I., Christaki, U., Mazzocchi, M. G., Montresor, M., Ribera d'Alcalá, M., Vaqué, D., and Zingone, A.: Plankton in the open Mediterranean Sea: a review, Biogeosciences, 7, 1543–1586, doi:10.5194/bg-7-1543-2010, 2010.

Stavrakakis, S. and Lykousis, V.: Interannual mass flux variations of settling particles in the NESTOR basins, SE Ionian Sea (E Mediterranean), Greece, Nucl. Instrum. Meth A, 626–627, 99–101, doi:10.1016/j.nima.2010.04.076, 2011.

Stavrakakis, S., Chronis, G., Tselepides, A., Heussner, S., Monaco, A., and Abassi, A.: Downward fluxes of settling particles in the deep Cretan Sea (NE Mediterranean), Prog. Oceanogr., 46, 217–240, doi:10.1016/s0079-6611(00)00020-3, 2000.

Suess, E.: Particulate organic carbon flux in the oceans – surface productivity and oxygen utilization, Nature, 288, 260–263, 1980.

Susumu, H.: Material fluxes and modes of sedimentation in the mesopelagic and bathy pelagic zones, J. Mar. Res., 38, 53–97, 1980.

Taillandier, V., D'Ortenzio, F., and Antoine, D.: Carbon fluxes in the mixed layer of the Mediterranean Sea in the 1980s and the 2000s, Deep-Sea Res. Pt. I, 65, 73–84, doi:10.1016/j.dsr.2012.03.004, 2012.

Takahashi, K., Fujitani, N., Yanada, M., and Maita, Y.: Long-term biogenic particle fluxes in the Bering Sea and the central subarctic Pacific Ocean, 1990–1995, Deep-Sea Res. Pt. I, 47, 1723–1759, 2000.

Takahashi, K., Fujitani, N., and Yanada, M.: Long term monitoring of particle fluxes in the Bering Sea and the central subarctic Pacific Ocean, 1990–2000, Prog. Oceanogr., 55, 95–112, 2002.

Theocharis, A., Nittis, K., Kontoyiannis, H., Papageorgiou, M., and Balopoulos, E.: Climatic changes in the Aegean Sea influence the Eastern Mediterranean thermohaline circulation (1986–1997), Geophys. Res. Lett., 26, 1617–1620, 1999.

Theodosi, C., Parinos, C., Gogou, A., Kokotos, A., Stavrakakis, S., Lykousis, V., Hatzianestis, J., and Mihalopoulos, N.: Downward fluxes of elemental carbon, metals and polycyclic aromatic hydrocarbons in settling particles from the deep Ionian Sea (NESTOR site), Eastern Mediterranean, Biogeosciences Discuss., 9, 19165–19197, doi:10.5194/bgd-9-19165-2012, 2012.

Thingstad, T. F. and Rassoulzadegan, F.: Nutrient limitations, microbial food webs, and biological C-pumps: suggested interactions in a P-limited Mediterranean, Mar. Ecol.-Prog. Ser., 117, 299–306, 1995.

Touratier, F. and Goyet, C.: Impact of the Eastern Mediterranean Transient on the distribution of anthropogenic CO_2 and first estimate of acidification for the Mediterranean Sea, Deep-Sea Res. Pt. I, 58, 1–15, doi:10.1016/j.dsr.2010.10.002, 2011.

Triantaphyllou, M. V., Ziveri, P., and Tselepides, A.: Coccolithophore export production and response to seasonal surface water variability in the oligotrophic Cretan Sea (NE Mediterranean), Micropaleontology, 50, 127–144, doi:10.2113/50.Suppl_1.127, 2004.

Trimonis, E. and Rudcnko, M.: Geomorphology and bottom sediments of the Pylos area, in: Proceedings of the 2nd NESTOR International Workshop, edited by: Resvanis, L. K., p. 321, 1992.

Verardo, D. J., Froelich, P. N., and McIntyre, A.,: Determination of organic carbon and nitrogen in marine sediments using the Carlo Erba NA-1500 Analyzer, Deep-Sea Res., 37, 157–165, 1990.

Verdugo, P., Alldredge, A. L., Azam, F., Kirchman, D. L., Passow, U., and Santschi, P. H.: The oceanic gel phase: a bridge in the DOM-POM continuum, Mar. Chem., 92, 67–85, 2004.

Volk, T. and Hoffert M.: Ocean carbon pumps: analysis of relative strengths and efficiencies in ocean-driven atmospheric CO_2 changes, in: The Carbon Cycle and Atmospheric CO_2: Natural Variations Archean to Present, Geophys. Monogr. Ser., vol. 32, edited by: Sundquist, E. T. and Broecker, W. S., 99–110, AGU, Washington, DC, doi:10.1029/GM032p0099, 1985.

Wakeham, S. G. and Lee, C.: Production, transport, and alteration of particulate organic matter in the marine water column, in: Organic Geochemistry, edited by: Engel, M. H. and Macko, S. A., 145–169, Plenum Press, 1993.

Wong, C. S., Whitney, F. A., Crawford, D. W., Iseki, K., Matear, R. J., Johnson, W. K., Page, J. S., and Timothy, D.: Seasonal and interannual variability in particle fluxes of carbon, nitrogen and silicon from time series of sediment traps at Ocean Station P, 1982–1993: relationship to changes in subarctic primary productivity, Deep-Sea Res. Pt. II, 46, 2735–2760, 1999.

BGD

10, 591–641, 2013

Yokokawa, T., De Corte, D., Sintes, E., and Gerndl, G. J.: Spatial patterns of bacterial abundance, activity and community composition in relation to water masses in the Eastern Mediterranean Sea, Aquat. Microb. Ecol., 59, 185–195, 2010.
Zuniga, D., Calafat, A., Sanchez-Vidal, A., Canals, M., Price, B., Heussner, S., and Miserocchi, S.: Particulate organic carbon budget in the open Algero-Balearic Basin (Western Mediterranean): assessment from a one-year sediment trap experiment, Deep-Sea Res. Pt. I, 54, 1530–1548, 2007.

BGD
10, 591–641, 2013

Table 1. Time weighted mean fluxes ($mg\,m^{-2}\,d^{-1}$) and flux weighted mean content (percentage of dry weight) for each sediment trap. Numbers in brackets indicate the total mass fluxes used for determination of flux weighted mean percentages and time weighted mean fluxes of major constituents. Underlined time weighted mean fluxes indicate values for the common collecting period 1 November 2006 to 15 March 2010.

Depth	Total mass flux	Organic Carbon		Carbonate		Biogenic Silica		Lithogenic	
		%	flux	%	flux	%	flux	%	flux
700	65.58	3.89	2.55	28.29	22.66	10.15	7.18	51.70	33.82
	65.58		(65.58)		(76.44)		(70.73)		(65.41)
1200	58.07	3.45	2.00	29.64	20.96	12.06	7.46	51.45	38.09
	63.55		(58.07)		(70.71)		(61.87)		(74.04)
2000	53.74	3.05	1.64	28.49	17.61	12.20	6.56	53.21	32.89
	56.46		(53.74)		(61.81)		(53.74)		(61.81)
3200	34.25	3.20	1.10	26.41	8.82	12.98	5.05	52.00	18.65
	33.90		(34.25)		(33.38)		(38.91)		(35.87)
4300	52.27	2.85	1.49	28.56	18.98	10.70	6.08	55.10	38.43
	55.97		(52.27)		(66.45)		(56.79)		(69.76)

BGD
10, 591–641, 2013

Table 2. Descriptive statistics of total mass and main constituent fluxes ($mg\,m^{-2}\,d^{-1}$), and contribution (%) of main constituents to total mass for the different traps.

Trap		Total	Organic Carbon		Carbonate		Opal		Lithogenic	
(m)		mass flux	%	flux	%	flux	%	flux	%	flux
700	Min	0.62	2.08	0.08	15.93	0.34	3.45	0.25	32.57	1.52
	Max	484.37	15.79	12.97	46.96	126.56	16.98	50.16	64.00	282.14
	.Mean	65.58	3.89	2.55	28.29	22.66	10.15	7.18	51.70	33.82
	Std. Dev.	92.44	2.92	2.80	6.51	25.32	2.913	9.615	7.76	59.26
	C.V. (%)	140.96	75.23	111.55	23.03	111.74	28.70	133.91	14.43	175.22
1200	Min	1.93	2.21	0.16	16.46	0.33	3.61	0.11	36.43	1.13
	Max	296.70	10.83	12.29	46.96	93.94	22.90	67.93	69.71	160.94
	.Mean	58.07	3.45	2.00	29.64	20.96	12.06	7.46	51.45	38.09
	Std. Dev	72.05	2.25	2.33	5.70	22.14	3.69	11.39	7.81	39.62
	C.V. (%)	124.07	65.15	116.50	19.13	105.63	30.61	152.68	15.18	104.02
2000	Min	2.88	1.74	0.09	20.08	0.07	6.25	0.38	40.91	1.45
	Max	331.95	10.27	11.35	38.99	82.25	24.12	71.28	67.10	159.04
	.Mean	53.74	3.05	1.64	28.49	17.61	12.20	6.56	53.21	32.89
	Std. Dev	63.29	1.52	1.89	4.29	16.11	3.23	11.09	5.93	35.17
	C.V. (%)	117.77	49.78	115.24	15.06	91.48	26.48	169.06	11.14	106.93
3200	Min	0.46	1.88	0.03	12.99	0.27	4.43	0.31	40.28	1.021
	Max	222.53	7.87	7.73	37.21	59.74	29.31	50.11	70.32	97.22
	Mean	34.25	3.20	1.10	26.41	8.82	12.98	5.05	52.00	18.65
	Std. Dev	38.90	1.26	1.30	4.86	11.28	4.27	8.10	6.30	21.44
	C.V. (%)	113.58	39.46	118.18	18.39	127.89	32.90	160.40	12.12	112.50
4300	Min	0.12	0.06	0.01	11.56	0.79	6.06	0.160	42.20	2.08
	Max	303.36	16.86	9.66	54.93	78.61	15.93	47.90	73.96	166.13
	.Mean	52.27	2.85	1.49	28.56	18.98	10.70	6.08	55.10	38.43
	Std. Dev	63.09	2.85	1.77	6.40	19.05	2.26	8.33	6.21	38.02
	C.V. (%)	120.71	99.97	118.79	22.39	100.37	21.12	137.01	11.27	98.93

BGD
10, 591–641, 2013

Table 3. A summary of seasonally compiled fluxes of total mass for the period 2006–2010. The definitions of the seasons are as follows: Winter: January–March; Spring: April–June; Summer: July–September; and Autumn: October–December.

		700 m	1200 m	2000 m	3200 m	4300 m
2006						
	Winter					
	Spring					48.32
	Summer		12.87	31.82	44.86	31.29
	Autumn	9.31	7.57	19.49	34.90	5.34
2007						
	Winter	11.98	5.95	9.12	26.76	2.35
	Spring	24.85	65.19	42.01	56.42	30.44
	Summer	19.26	40.68	40.61	57.97	53.51
	Autumn	40.45	11.33	19.74	18.66	33.96
2008						
	Winter	38.22	12.18	8.12	5.81	9.16
	Spring	129.99	73.28	123.57	28.09	84.76
	Summer	109.88	133.33	79.40	20.44	41.51
	Autumn					
2009						
	Winter					
	Spring	130.33	191.20	199.45	124.87	217.65
	Summer	29.81	59.27	46.77	11.15	122.75
	Autumn	2.32	4.84	21.89	3.25	4.29
2010						
	Winter	201.31	97.59	50.24	8.15	11.02

BGD
10, 591–641, 2013

Table 4. Comparison of organic carbon fluxes measured with sediment traps and the corresponding export ratios with the organic carbon fluxes and export ratios obtained by empirical equations. Numbers in brackets are the export ratios (%), primary production and fluxes in $mg\,m^{-2}\,d^{-1}$.

Depth (m)	Organic carbon flux[a]	Martin[b]	Betzer[c]	Suess[d]	Pace[e]
		241PP			
100		36.15 (15FR)	49.14 (20.39FR)	92.98 (38.58FR)	28.90 (11.99FR)
700	2.58 (1.07)	2.58 (1.87)	14.48 (6.01)	14.28 (5.93)	6.93 (2.87)
1200	2.18 (0.90)	1.45 (1.05)	10.32 (4.28)	8.38 (3.48)	4.66 (1.94)
2000	1.74 (0.72)	0.84 (0.35)	7.49 (3.11)	5.04 (2.09)	3.21 (1.33)
3200	1.12 (0.46)	0.51 (0.21)	5.57 (2.31)	3.16 (1.31)	2.27 (0.94)
4300	1.63 (0.68)	0.37 (0.15)	4.63 (1.92)	2.35 (0.98)	1.83 (0.76)
4500B[f]		0.35 (0.15)	4.50 (1.87)	2.25 (0.93)	1.77 (0.73)

PP: Primary production (Colella et al., 2004)
FR: f-ratio (organic carbon flux/primary production % at 100 m).
[a] Measured with sediment traps.
[b] Estimated by modified Martin's equation, $b = -1.07$ (see text).
[c] $F_z = 0.388 \times z^{-0.628} \times PP^{1.41}$ (Betzer et al., 1984).
[d] $F_z = PP \times (0.0238 \times z + 0.212)^{-1}$ (Suess, 1980).
[e] $F_z = PP \times 3.523 \times z^{-0.734}$ (Pace et al., 1987).
[f] Bottom.

Discussion Paper | Discussion Paper | Discussion Paper | Discussion Paper |
BGD
10, 591–641, 2013
Downward fluxes of sinking particulate matter in the deep Ionian Sea
S. Stavrakakis et al.

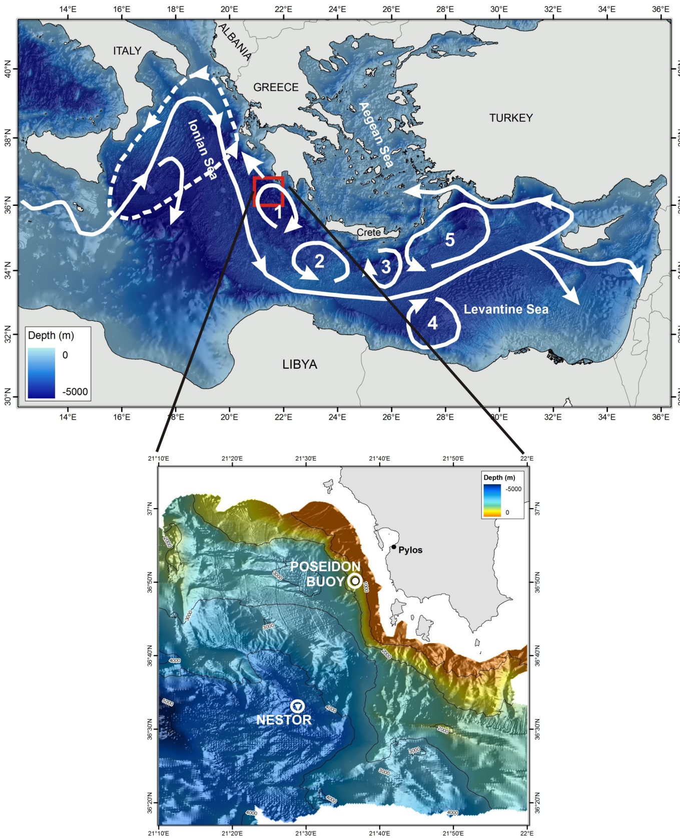

Fig. 1. Study area and location of the sampling sites in the southeast Ionian Sea (Eastern Mediterranean). Schematic of the general circulation in the Eastern Mediterranean in the upper 500 m is also presented: 1, 2, 3, 4, 5 indicate the Pelops anticyclone, the Cretan cyclone, the Ierapetra anticyclone, the Mersha-Matruh gyre, and the Rhodes gyre, respectively. Dotted loop indicates the north Ionian gyre circulation, whenever it occurs.

BGD
10, 591–641, 2013

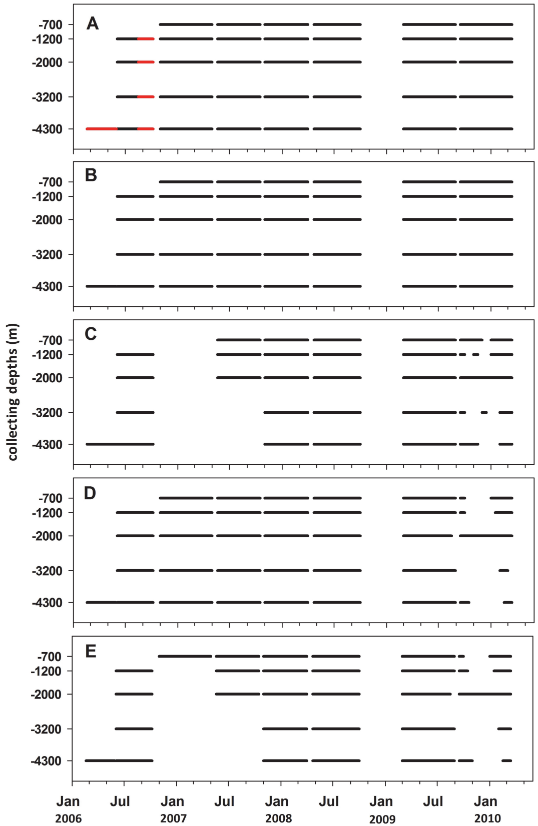

Fig. 2. (A) Duration and time and depth coverage of NESTOR trap sampling. The red lines indicate one week sampling interval, while the black lines two week sampling interval. **(B–E)**: time-slots for organic carbon, carbonates, opal and lithogenic (respectively) analyzed in this study.

BGD
10, 591–641, 2013

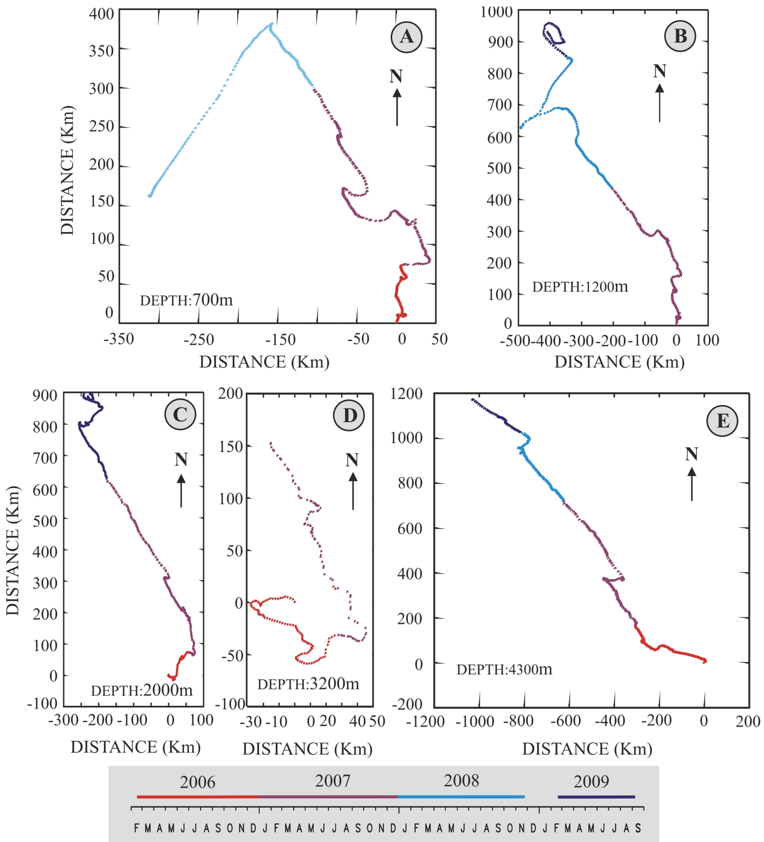

Fig. 3. Progressive vector diagrams (left panels) based on unfiltered current meter data at the various depths of measurements on the mooring at NESTOR site. Corresponding colored lines below indicate the duration and time coverage of the current record for the specific year they refer to.

BGD

10, 591–641, 2013

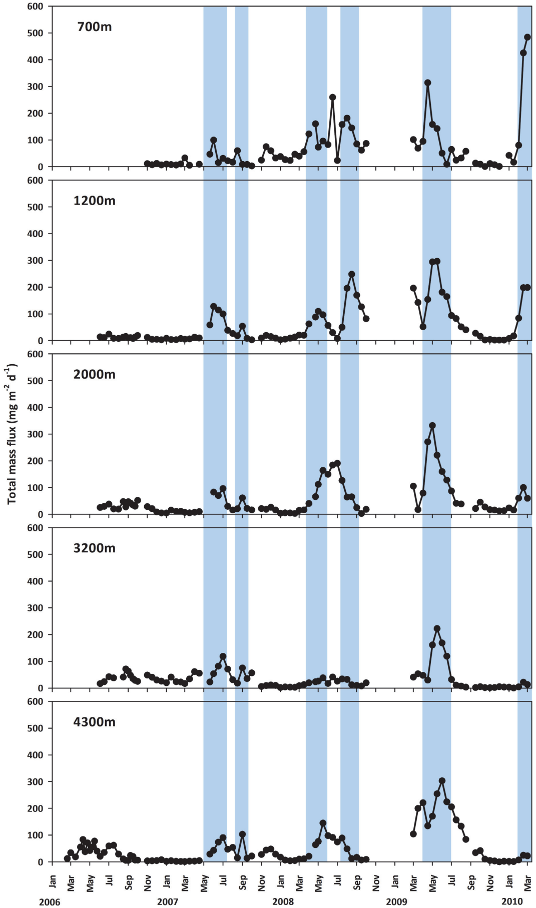

Fig. 4. Time-series plots of total mass flux ($mg\,m^{-2}\,d^{-1}$) of downward settling particles collected by sediment traps during the course of the long-term experiment in NESTOR site.

BGD
10, 591–641, 2013

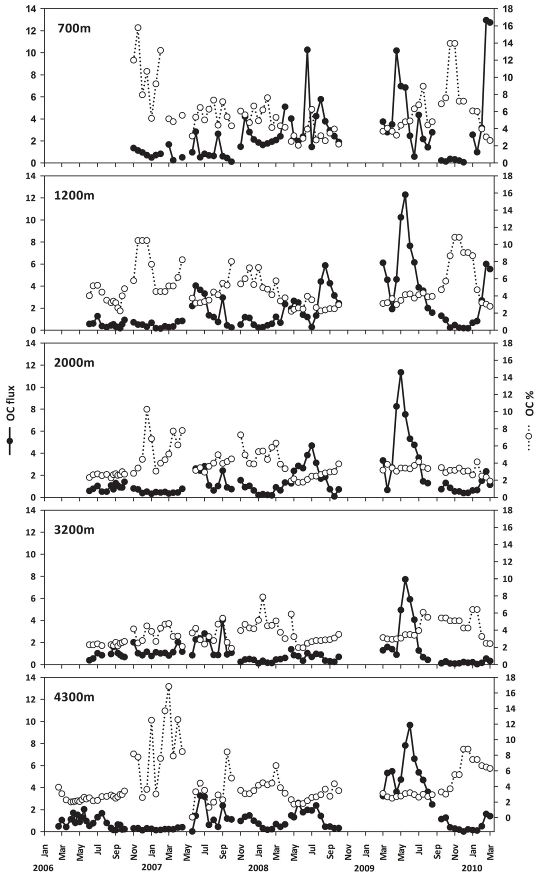

Fig. 5. Time-series plots of organic carbon content (%) and fluxes ($mg\,m^{-2}\,d^{-1}$) of downward settling particles collected by sediment traps during the course of the long-term experiment in NESTOR site.

BGD
10, 591–641, 2013

Downward fluxes of sinking particulate matter in the deep Ionian Sea

S. Stavrakakis et al.

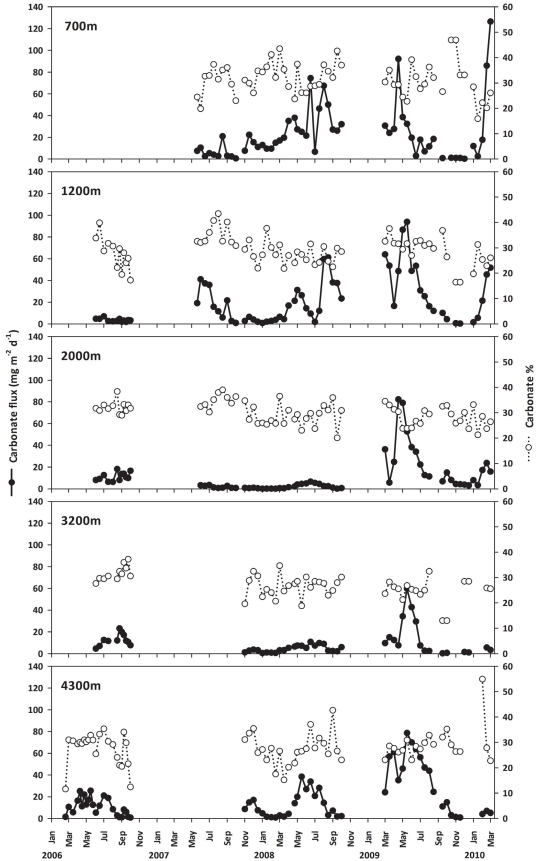

Fig. 6. Time-series plots of carbonate content (%) and fluxes (mg m^{-2} d^{-1}) of downward settling particles collected by sediment traps during the course of the long-term experiment in NESTOR site.

BGD
10, 591–641, 2013

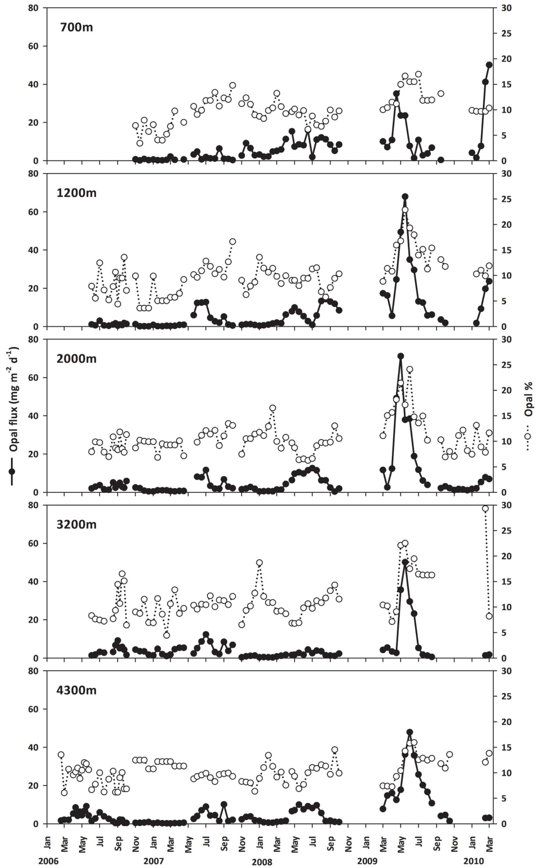

Fig. 7. Time-series plots of opal content (%) and fluxes (mg m^{-2} d^{-1}) of downward settling particles collected by sediment traps during the course of the long-term experiment in NESTOR site.

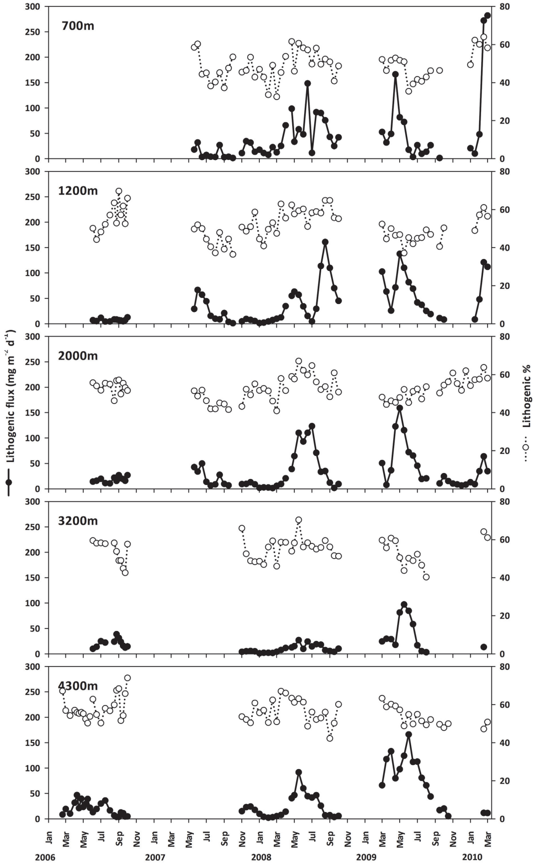

Fig. 8. Time-series plots of lithogenic fraction content (%) and fluxes ($mg\,m^{-2}\,d^{-1}$) of downward settling particles collected by sediment traps during the course of the long-term experiment in NESTOR site.

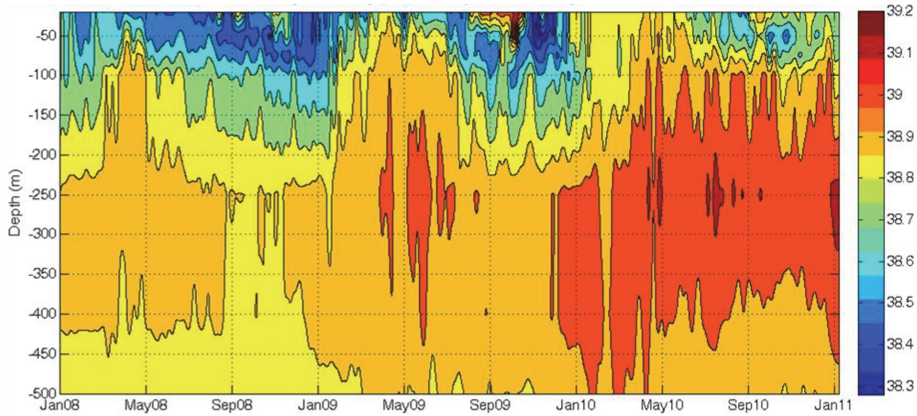

Fig. 9. Time-depth contour plot of the salinity evolution in the upper 500 m as recorded by the Poseidon buoy (shown in Fig. 4 with a cross) at NESTOR site.

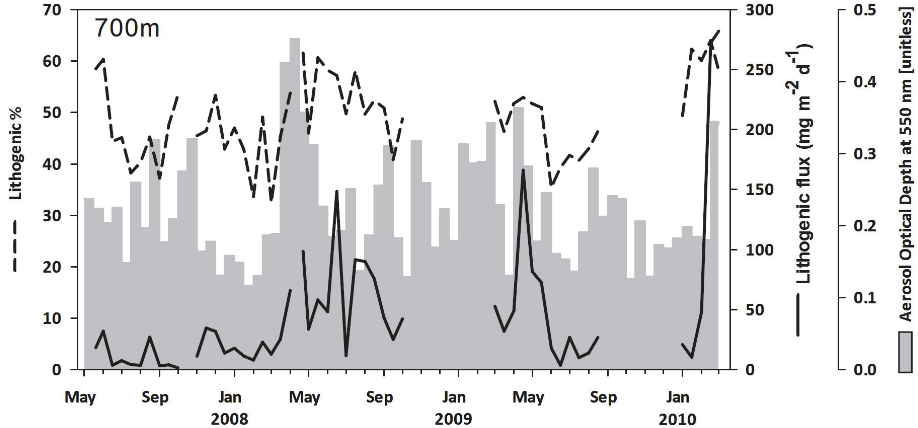

Fig. 10. Time series plot of lithogenic content and flux, and aerosol optical depth at 550 nm. Analyses of aerosol optical depth used in this plot were produced with the Giovanni online data system, developed and maintained by the NASA GES DISC.

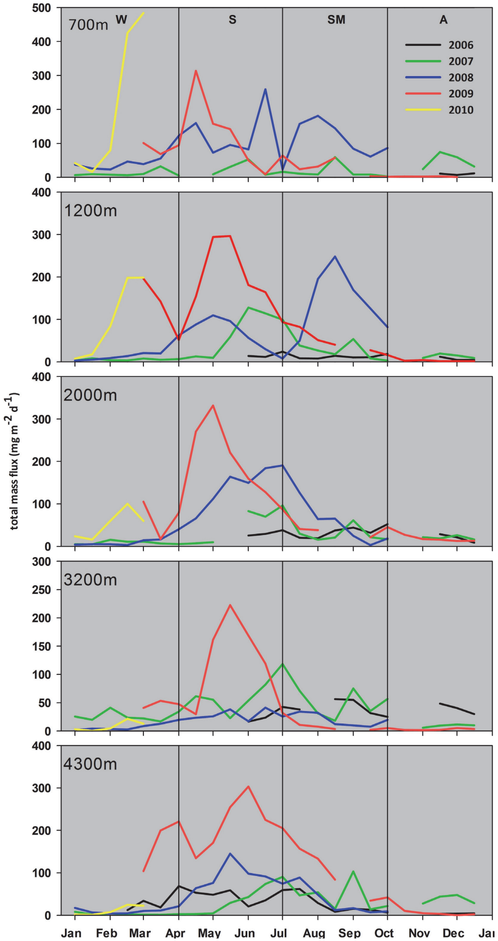

Fig. 11. Multi-year plots of total mass fluxes at NESTOR site (2006–2010). w: winter, s: spring, sm: summer, a: autumn.

BGD

10, 591–641, 2013

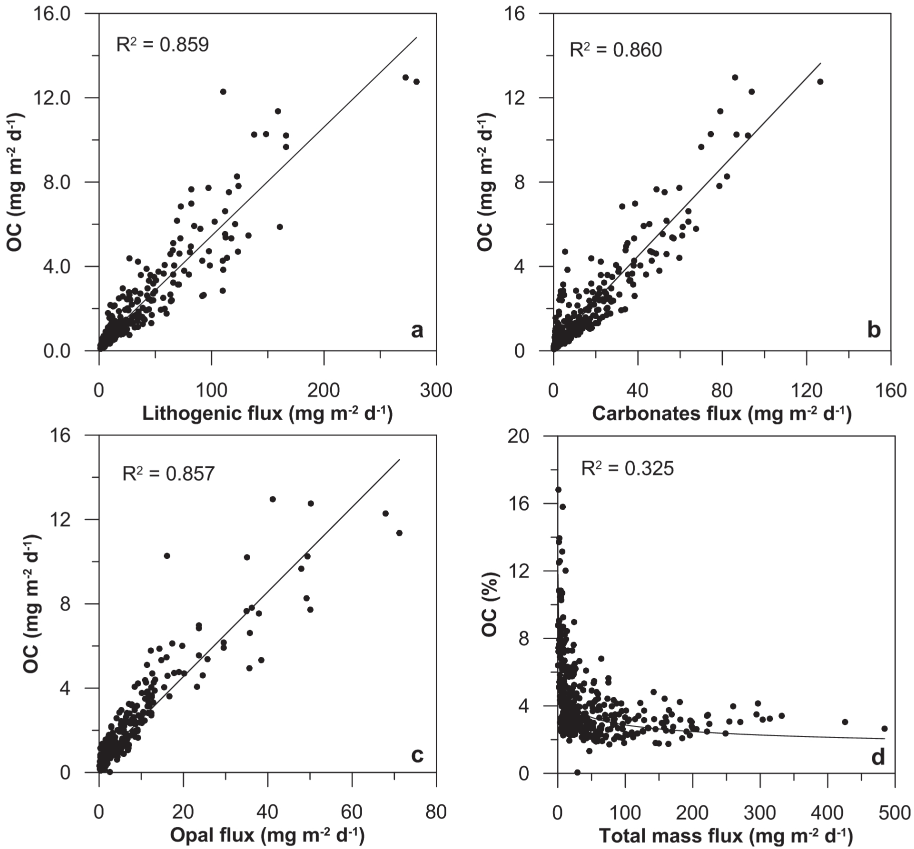

Fig. 12. Organic carbon flux vs. **(a)** lithogenic flux; **(b)** carbonate flux; **(c)** opal flux; and **(d)** organic carbon content vs. total mass flux.

BGD

10, 591–641, 2013